North Atlantic Ocean surface currents

Gilles Reverdin[1]

Centre National d'Etudes Spatiales/Centre National de la Recherche Scientifique/Université Paul Sabatier, UMR5566, Toulouse, France

P. P. Niiler

Scripps Institution of Oceanography, University of California, San Diego, La Jolla, California, USA

H. Valdimarsson

Marine Research Institute, Reykjavik, Iceland

Received 12 June 2001; revised 27 December 2001; accepted 5 January 2002; published 3 January 2003.

[1] Close to 1800 surface drifters are used to investigate the 15 m circulation of the North Atlantic Ocean. The data are used to describe structures of the average Eulerian circulation and of the associated eddy variability. The data resolve scales on the order of 50 km, which have hitherto not been systematically described, in particular, near shelf breaks and near the most intense currents, the Gulf Stream, the North Atlantic Current (NAC), and the frontal currents of the subpolar gyre. This reveals a complex series of quasi-permanent eddies, meanders, and recirculation patterns. Gulf Stream intensity is portrayed as changing abruptly near 54°W, east of which, it is identified as two current branches centered near 39° and 41.5°N, the northern one connecting more directly with the NAC, and the southern one with the recirculation gyre and the Azores Current (AC). Many features of the currents are controlled by topography, in particular, currents are often intensified near shelf breaks or parallel to ridges in the subpolar gyre. However, the largest northward branch of the NAC in the Icelandic basin is located near the deepest bathymetry, not near steep bathymetry. Other currents, in particular, in the subtropical gyre, are less clearly related to topography: for instance, the AC is featured as a zonal eastward current extending far west of the Mid-Atlantic Ridge (MAR) to at least 55°W and possibly 63°W. In the interior and away from topographic features the eddy kinetic energy (EKE) is the largest where the mean currents are the largest. In the subpolar gyre, there are striking differences in EKE between southward flowing currents (the Labrador and east Greenland Current) and the northward flowing currents (west Greenland Current and branches of the NAC), which have higher EKE. The areas of weakest variability are located in the southwest part of the subpolar gyre, northeast of Iceland, and in the eastern Atlantic south of 45°N. The AC eddies and the mesoscales south of the Canary Islands transect this eastern eddy desert. Drifter trajectories are used as realizations of Lagrangian particles in the vicinity of current cores. These illustrate the variety of paths or connections between different current systems and demonstrate cross-stream dispersions. *INDEX TERMS:* 4512 Oceanography: Physical: Currents; 4532 Oceanography: Physical: General circulation; 4576 Oceanography: Physical: Western boundary currents; *KEYWORDS:* surface currents, North Atlantic Ocean

Citation: Reverdin, G., P. P. Niiler, and H. Valdimarsson, North Atlantic Ocean surface currents, *J. Geophys. Res.*, *108*(C1), 3002, doi:10.1029/2001JC001020, 2003.

1. Introduction

[2] We will describe the horizontal currents at 15 m in the North Atlantic estimated from buoy drifts mostly in the 1990s. Eulerian maps of the currents and of eddy kinetic energy (EKE) are derived, and we present a rudimentary description of the horizontal dispersion of surface water from the trajectories in areas of major currents. The number of drifters deployed is quite large compared to the other oceans and provides an opportunity to resolve scales that are difficult to resolve by other observing systems.

[3] We follow the classical approach where buoy drifts are used to map the average currents as well as other Eulerian statistics. We will refer to this as the quasi-Eulerian approach as was done for mapping the near-surface Atlantic currents, in particular, by *Richardson* [1983] and *Brügge*

[1]Now at Laboratoire d' Océanographie Dynamique et de Climatologie, CNRS, Université Paris VI, Paris, France.

0148-0227/03/2001JC001020

Table 1. Drifter Data Sources in the North Atlantic

	Type	Source/Processing	Drogue	Time Period
1196	SVP	AOML/DDC	@15 m	31 October 1989 to 1 June 2000
1247	SVP	AOML/DDC	none	17 Feb. 1990 to 1 June 2000
314	CMOD	MEDS/SIO	none	1 Jan. 1990 to 29 June 2000
48	SVP	Dunstable Lab/SIO	@40 m	23 May 1995 to 5 May 1997
24	SVP	University of Lisbon/SIO	@15 m	14 Jan. 1993 to 21 Oct. 1994
113	FGGE	USCG/URI	@50 m	22 Sept. 1977 to 10 Nov. 1993

[1995], as well as in many regional studies. The implicit hypothesis is that the drifters, as they move randomly, sample a space and time variable field of currents. Biases can originate from the inhomogeneity of the float distribution [*Davis*, 1991] and from the presence of an average spatial structure of EKE [*Freeland et al.*, 1975]. It is also likely that horizontally convergent structures will be more sampled than divergent ones, which will result in biases when this correlates with differences in the currents [*Davis*, 1998]. This is a particular issue in the vicinity of surface fronts or in areas where the horizontal convergence varies at low frequencies, with the result that some periods will be better sampled than others (for example, a seasonal cycle, as is observed close to the surface near the equator).

[4] A comparison between quasi-Eulerian and Eulerian estimates of the Atlantic Ocean circulation in a high-resolution Miami Isopycnic Coordinate Ocean Model (MICOM) simulation has been presented by *Garraffo et al.* [2001b], which suggests that differences related to these effects might not be critical, at least outside of the tropical Atlantic. Also, drifters do not follow water motion precisely because of wind slip so the tendencies to remain in convergent zones are partially eliminated. Furthermore, the systematic errors in the quasi-Eulerian approach to the mean circulation were usually found to be small in front of the rms uncertainty because of the sampling, except possibly in intense western boundary currents. This study also suggests that EKE is well estimated by the quasi-Eulerian approach.

[5] EKE is an important product of the quasi-Eulerian mapping. The major currents are expected to be a main source of EKE through their instabilities. It is usually assumed in analyses of time variable altimetric sea level at midlatitudes away from topography that areas of high EKE correspond to areas of energetic currents. A conclusion is then made that changes in the patterns of EKE are indicative of changes in the strong current systems [e.g., *White and Heywood*, 1995]. We discuss here, using the quasi-Eulerian maps, how the distribution of EKE relates to the average currents. EKE in the North Atlantic has been estimated also from moorings [*Wunsch*, 1997] and from altimetric slopes, either for the velocity component perpendicular to the satellite tracks [*Stammer*, 1997] or from mapped sea level [*Ducet et al.*, 2000]. *Ducet et al.* [2000] estimates of EKE compare well with EKE mapped from the drifter data, although there is a difference in the ratio of meridional over zonal rms variability, which is smaller for the drifter composites than in the altimeter-derived estimates [see also *Fratantoni*, 2001]. This suggests that perhaps strong zonal portions of the mesoscale are convergent and drifters reside in these regions in a preferential fashion. In this study we will not resolve this important issue, which perhaps can be answered by seeding particles into high-resolution general circulation models. We cannot resolve this problem with drifter data only. The close correspondence of the total energy with other independent data sets gives us confidence that the data are sufficient to derive a statistical estimate of the sampling error. The confidence in the product is also reinforced by the similarity between estimates based on subsets of the drifters or data from specific seasons or years.

[6] It is only recently that surface drifters have been designed to be good current followers [*Niiler et al.*, 1987, 1995]; that is, they follow closely the currents at a given level, as can be checked by current meters attached to the float. Most of the data used in this analysis or in *Brügge* [1995] have this $O(1 \text{ cm s}^{-1})$ error in the drift. Other sources of differences with the larger-scale currents have, however, not yet been estimated: for example, Langmuir cells that are convergent and that extend to below 15 m depth could contribute to deviations of the buoy drifts from the large-scale ocean currents at the drogue level. In the North Atlantic the eddy energy is sufficiently large that the $1-5$ cm s^{-1} deviation due to these unresolved processes will not affect in a substantial fashion the results presented. All these contributions to the deviations of the drifts from the large-scale currents should be predominantly related to the wind and are likely included in the models of the wind (Ekman) component in the 15 m buoy drift [*Ralph and Niiler*, 1999]. This component of the drift is rather large scale for the present data and is usually small compared to the average drift. We will not discuss it further in this paper.

[7] In this paper we will first present the general characteristics of the data set in section 2, and then discuss the large-scale circulation and eddy fields revealed in the quasi-Eulerian maps and from the trajectories in section 3. We discuss the 15 m regional circulation in key areas of the North Atlantic in section 4.

2. North Atlantic Drifter Data

2.1. Drifter Description

[8] The drifter data in the North Atlantic came from two different instruments, the Surface Velocity Program (SVP) and the Canadian Meteorological Ocean Drifter (CMOD) (Table 1). Most of the drifter data were from the SVP drifters that consisted of a $25-40$ cm diameter spherical plastic surface float, which was tethered to a $6-7$ m long, 1 m diameter holey sock drogue, centered at $15-50$ m depth [*Sybrandy and Niiler*, 1991]. Field observations with current meters attached to the drogue demonstrated that the SVP drifter with a drogue attached slips down wind at 0.12 cm s^{-1} m^{-1} s^{-1} wind at 10 m [*Niiler et al.*, 1995]. A complete Metafile on the construction of each SVP drifter with a 15 m drogue is compiled at the Global Drifter Center at Atlantic Oceanographical and Meteorological Laboratory (AOML). The Marine Environmental Data Service (MEDS, Canada) is the responsible data center for Argos drifter data.

[9] The half-life of the SVP drogues was 170–550 days, depending when they were made and the severity of sea conditions where they were deployed [*Poulain and Niiler*, 1990; *Sybrandy and Niiler*, 1991]. When the drogue was attached, the surface float was pulled under water, and a pair of electrical seawater contacts on the upper portion of the float registered a closed circuit. The number of closures in a fixed time period was compiled and sent via Service Argos Data Collection and Location System (ARGOS) as a data file. When the drogue became detached, the float did not submerge, and very few closures were registered. Some drifters upon deployment did not record submergence at all because of seawater circuit malfunction. When the submergence was not recorded, the data were treated as having no drogue after 170 days, the most conservative estimate of the drogue half-life. Some drifters were deployed without a drogue sensor, and again, these drifters were assumed to have lost a drogue after 170 days. Drift data from SVP drifters that had lost their drogues were compared with data of drifters with drogues attached. The undrogued SVP drifters slip down wind 0.88 cm s^{-1} m^{-1} s^{-1} National Centers for Environmental Prediction (NCEP) reanalysis 10 m wind with respect to the SVP drifters with drogues attached [*Pazan and Niiler*, 2001].

[10] The CMOD drifter consisted of a 61 cm long, 12 cm diameter cylindrical canister that was kept afloat by a nitrogen filled, doughnut-shaped airbag around the canister. Upon deployment the deployment canister outer shell settles at a specified depth, attached by a nylon filament. A 55 cm long mast popped up from the top of the canister for sensing air pressure. There was no sensor to indicate whether the drogue element was attached. The half-life of CMODs' transmissions to ARGOS was 40 days. Drift data from CMODs, when compared with the SVPs with drogues, indicated that CMODs slip downwind relative to the SVPs with drogues at 0.88 cm s^{-1} m^{-1} s^{-1} NCEP reanalysis 10 m wind [*Pazan and Niiler*, 2001].

[11] The United States Coast Guard (USCG) Ice Patrol has been releasing drifters within the iceberg drift area of the Labrador Current in the spring and early summer seasons. These data were processed and graciously provided to us by the University of Rhode Island (URI). *Carr and Rossby* [2001] discuss aspects of the relationships of the USCG data to deep float trajectories. USCG-deployed drifters of the design developed under the first Global Garp Experiment (FGGE) [*Garrett*, 1980] and are of various shapes, sizes, and modes of attachment of various drogues at 50 m depth to floats of various shapes and sizes. We include this data (first 180 days) in our description with some reservations but feel that such a large number of deployments do improve the description of the eddy energy of an area where the more carefully calibrated SVPs did not produce as many observations.

2.2. Data Processing

[12] The drifter locations were provided by Service ARGOS from the ARGOS Doppler ranging system on NOAA Nimbus polar-orbiting satellites. The accuracy of these locations depended upon the "quality" and number of the radio transmissions received by ARGOS, and drifters were typically located within a radius that exceeds 250 m [*Poulain et al.*, 1996]. The data were placed on Global Telecommunication System (GTS) and sent to either AOML Drifter Data Center (DDC) or to the principal investigator of a particular drifter project. DDC interpolated the unevenly sampled locations to uniform 6 hourly locations by kriging and also provided an estimate of the 6 hourly velocity by center differencing the location data in time [*Hansen and Poulain*, 1996]. We also obtained the raw data files from the drifter data not accessed by DDC (Table 1) and processed these into 6 hourly samples. For interpolation we used either a model of the autocorrelation function derived with Fourier spectral methodology [*Van Meurs and Niiler*, 1997] or by direct linear interpolation.

[13] A six hourly 10 m NCEP reanalysis wind vector was interpolated to each of the drifter locations. This wind vector was used to obtain a correction both for the wind-produced slip of drogues at 15 m or the slip of the undrogued SVP and for the CMOD floats relative to the SVP drifters with drogues. The correction for the slip of the six hourly data with attached drogues was a subtraction of a down wind slip of 0.12 cm s^{-1} m^{-1} s^{-1} of NCEP reanalysis six hourly wind. The correction for SVP drifters with drogues off and CMOD drifters was a subtraction of down wind slip velocity of 1.00 cm s^{-1} per 1 m s^{-1} of NCEP reanalysis 6 hourly wind. No wind slip corrections were applied to the SVP drifters with drogues at 40–50 m depth. These data form a significant number of the observations in the confluence of the North Atlantic Current and the Labrador Current system and the branch of the North Atlantic Current past Scotland as it enters the Norwegian Sea. Inferences based on these 40–50 m drogue data will be denoted throughout the analyses. The velocity time series were then filtered with a 2 day Lanczos filter to reduce inertial oscillation or inhomogeneities related to uneven time sampling of the locations (some drifters were on a 1 day on and 2 days off transmission mode).

2.3. Data Distribution and Mapping

[14] The release locations were not uniform in space and time. Noteworthy was the large number of concentrated releases in the coastal waters of Maine and New Jersey, the economic zone of southern Iceland, the continental shelf off Scotland, and the Azores Frontal Zone. Each of these concentrated releases was due to specific local experiments that made the data available to the AOML/DDC or directly to the investigators. We note from the tabulation of the principal data sources (Table 1) that the SVP drifter with a drogue at 15 m was the largest source of data. Nearly equal numbers of velocity estimates were due to drifters that either lost their drogue or had no drogue indicator (Figure 1). The number of drifters with a drogue at 40–50 m is smaller, with a significant contribution only in specific areas of the subpolar gyre. The spatial distribution of drifters with 15 m drogues on and the ones with no drogues are different, with the first one more concentrated in the areas near releases, whereas some areas farther away from launch sites, as in the eastern subtropical gyre, are more sampled by drogue-off drifters.

[15] The total density of wind-corrected observations presents few areas with insufficient data except in the eastern tropical Atlantic, in the Bahamas region, on the Labrador and North Sea shelves, and south of the Gulf Stream near Cape Hatteras (Figure 1). It is, however, far from uniform and rather patchy. A large gradient is found,

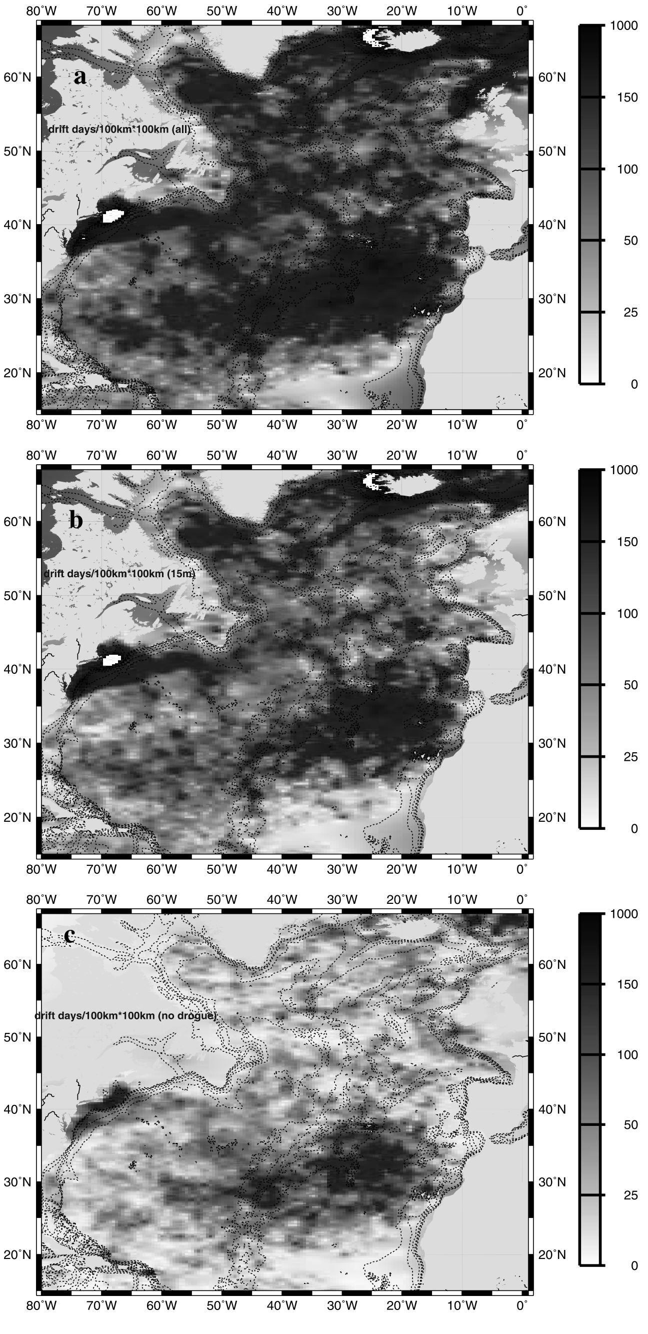

Figure 1. Data density (number of data days per 10^4 km^2): (a) the total density, (b) the data density for SVP drifters with drogue (excluding drifters drogued at 50 m near Scotland or in the Labrador Current by USGC), and (c) the data density for drifters without drogue (SVP and CMOD).

for example, across the Gulf Stream related to a larger number of buoys deployed north of the Gulf Stream, in the coastal waters of Maine and New Jersey. These inhomogeneities result in an array density bias of the estimated Eulerian velocity due to the particle diffusion that is estimated as the single-particle diffusivity times the observation density gradient [*Davis*, 1991]. With subsets of these data, estimates have been made of the single-particle diffusivities [*McClean et al.*, 2002] and diffusion-induced velocity bias [*Poulain et al.*, 1996]. We will discuss the magnitude of this effect in Appendix A.

[16] There are other biases. For example, more than 80% of the buoys in the Gulf Stream downstream of Cape Hatteras entered from the north usually after having drifted along the continental slope of the Mid-Atlantic Bight. When these drifters are entrained in the Gulf Stream, they are initially mostly north of the north wall of the Gulf Stream, and their velocity gradually increases during at least 1 day. We found, by giving less weight to these drifters (by a factor 10) than to other drifters, a significant change on the average currents in this area. In particular, the resulting average Gulf Stream was stronger close to Cape Hatteras and appeared to be more zonal downstream of the cape (see Appendix A).

[17] Mapping is usually done by grouping the filtered velocities on a fixed Eulerian grid, estimating mean and deviation statistics. Sampling uncertainties on those quantities are estimated independently on each grid box, but, of course, there is some correlation with nearby boxes because of time correlation of velocity along individual drifter tracks. The data set is complete enough that the sampling uncertainties can be tested by selecting subsets of the drifters or specific periods. This usually indicates (except when otherwise noted) that the features are robust for the period considered. The maps for the whole Atlantic have a resolution of 0.5° latitude and 1° longitude, and an average is produced when a minimum of 4 days of data are obtained from at least two drifters (at least 2° of freedom; note that we present an unbiased estimate of EKE). The averages are noisy in the few areas with marginal spatial coverage. In specific regions, a higher resolution can be picked that better resolves the scales of the average circulation and reduces the contribution of the subgrid scale of the mean flow to eddy statistics. Alternatively, in well-established currents, sections across the current are selected, and all trajectories crossing a particular portion of the section are grouped to estimate a velocity average. This allows in boundary currents a higher spatial resolution than what can be attained by the other method.

3. Large-Scale Circulation

[18] Fields derived include the average current on a 0.5° × 1° latitude × longitude grid, as well as σ_u and σ_v, which are the unbiased estimates of the standard deviation of the zonal and meridional velocity components in the bins. This also includes the average $\langle u'v' \rangle$, and EKE = $0.5*(\sigma_u^2 + \sigma_v^2)$.

[19] Characteristics of the large-scale circulation will be illustrated by the map of the mean velocity overlaying EKE (Figure 2). Portions of trajectories with particularly large velocities will illustrate what conditions are associated with high kinetic energy (the threshold will be either 1 or 0.5–1 m s^{-1} range, depending on the area; Figure 3). Maps are either shown in a rectangular projection or with a Mercator projection. We present therefore two sets of maps centered

Figure 2. (opposite) Map of EKE with average current and bathymetry (contours 200, 1000, 2000, 3000, and 4000 isobaths): (a) the northern and (b) the southern portions of the North Atlantic. The color scale is on the right. See color version of this figure at back of this issue.

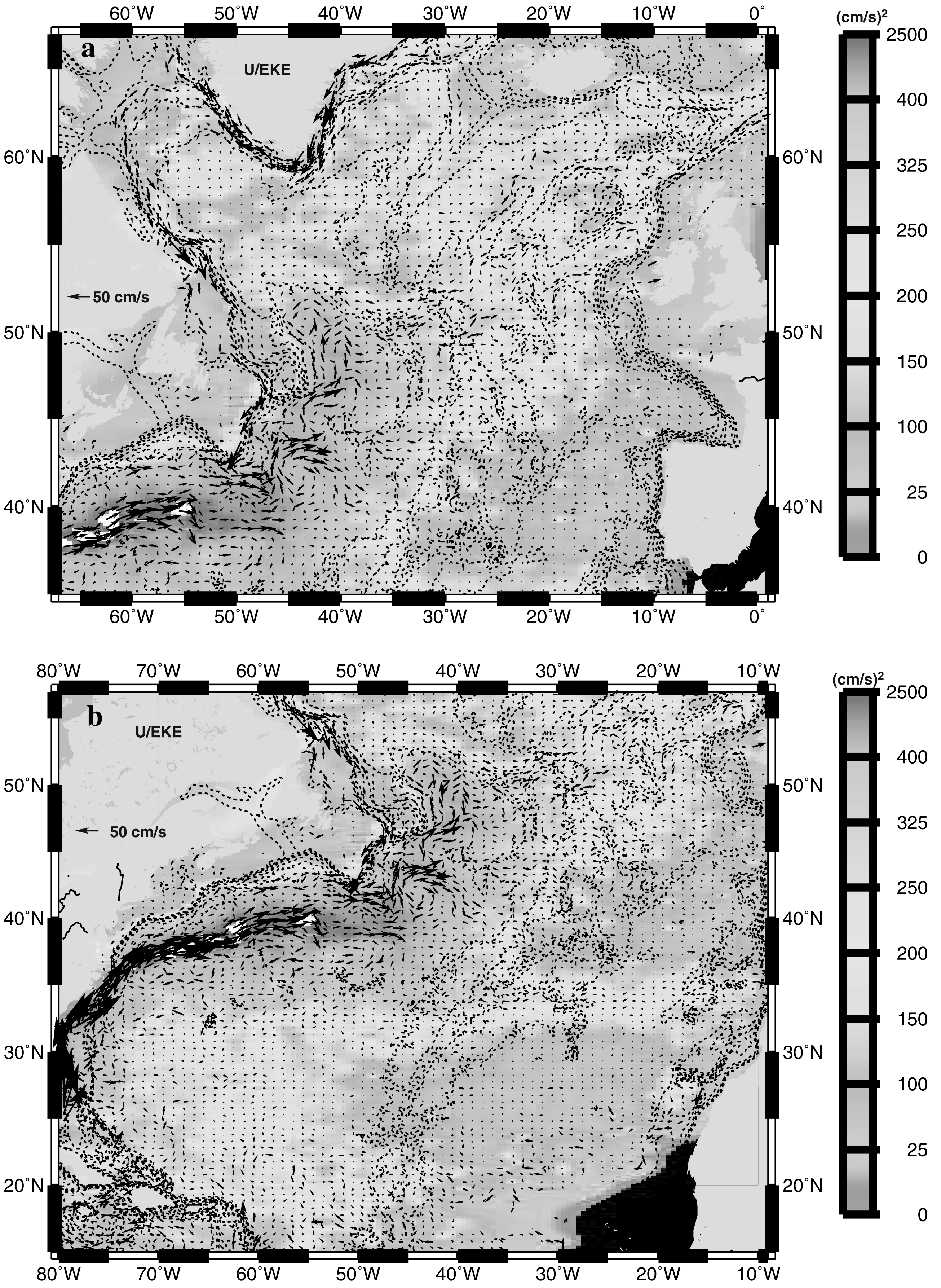
a
U/EKE
50 cm/s
60°W
50°W
40°W
30°W
20°W
10°W
0°
60°N
50°N
40°N
(cm/s)²
2500
400
325
250
200
150
100
25
0
b
U/EKE
50 cm/s
80°W
70°W
60°W
50°W
40°W
30°W
20°W
10°W
50°N
40°N
30°N
20°N
(cm/s)²
2500
400
325
250
200
150
100
25
0

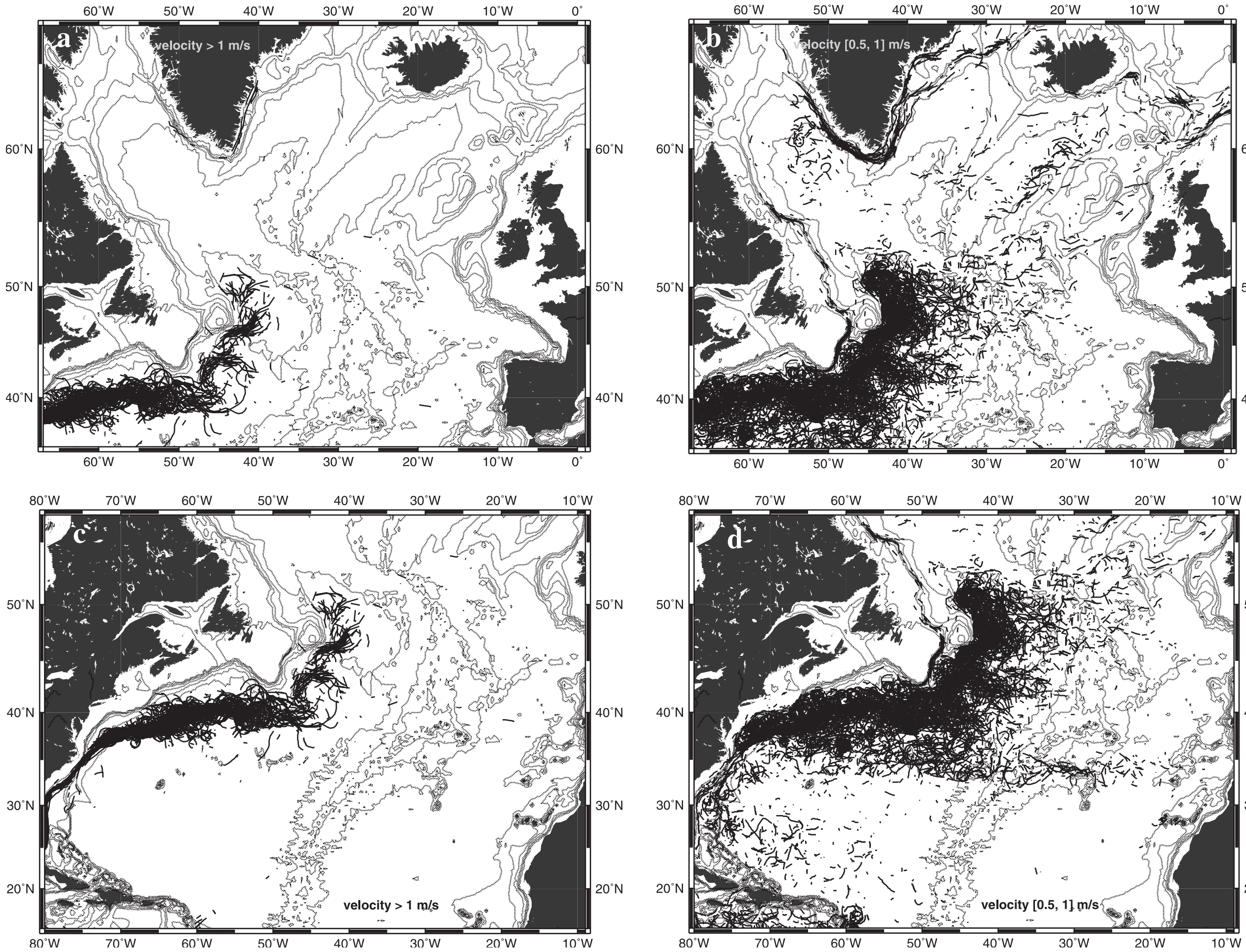

Figure 3. Trajectories corresponding to the velocity ranges 0.5–1 m s^{-1} and larger than 100 cm s^{-1} for the northern and the southern portions of the North Atlantic (after filtering velocity time series of individual drifters with a 2 day Lanczos filter).

on the subtropical and the subpolar gyre to limitate distortion. We will not include the Caribbean Sea and Gulf of Mexico (not yet as well sampled) as well as the Nordic Seas [see *Poulain et al.*, 1996].

[20] The largest mapped average currents (Figure 2) correspond roughly with the ones derived earlier from more limited drifter data in various special regions by a number of earlier studies [e.g., *Richardson*, 1983; *Krauss*, 1995; *Brügge*, 1995]. These can easily be identified as the western boundary currents (Labrador, east and west Greenland Currents, and Florida Current), and their continuations in the interior (Gulf Stream (GS), North Atlantic Current (NAC), the Azores Current (AC) and the branches of the NAC toward the northeast in the subpolar gyre) are prominent. To varying extents, recirculation patterns are associated with most of these currents. In association with the NAC occur the most intense and smallest-scale recirculation patterns as a series of semipermanent meanders and semiclosed eddies. The subpolar gyre south of the ridges separating it from the Nordic Seas is not portrayed as a continuous gyre but as an ensemble of domains separated by branches of current flowing to the northeast (from east to west: the Rockall Trough and Maury Channel branches and the Irminger Current west of the Reykjanes Ridge). The Irminger Current then forms the offshore branch of the east Greenland Current as it flows around Greenland toward the Labrador Sea.

[21] The GS west of 55°W is well defined but has a less clear path in these data farther east. Its connection with the NAC and other branches of eastward currents is not always clear. The data suggest that branches occur near 52° (only west of 27°W), 50.5°, 47°, and 34°N, although the exact position of these branches varies somewhat in subsets of the data. The flow between 47° and 34°N in the eastern Atlantic is quite weak, with a suggestion of southward flow. The current south of 33°N is usually weak and westward or southwestward, except in the vicinity of the Canaries Islands and toward the southern limit of the subtropical gyre (poorly sampled). The 15 m current in the western part of the subtropical gyre tends to have a northward component. There is evidence for the existence of eastward flow in an elusive subtropical front near 28°N west of 58°W. This eastward flow is also apparent in the relative dynamic height maps [*Stommel et al.*, 1978] and is further discussed in the literature of the FASINEX experiment [*Pollard and Regier*, 1992].

[22] The regions of highest EKE (Figure 2), often exceeding 2500 cm^{-2} s^{-2} between 53° and 70°W, are clearly associated with the GS, and the EKE also reaches 2000 cm^2 s^{-2} within the Florida Current north of 31°N and NAC

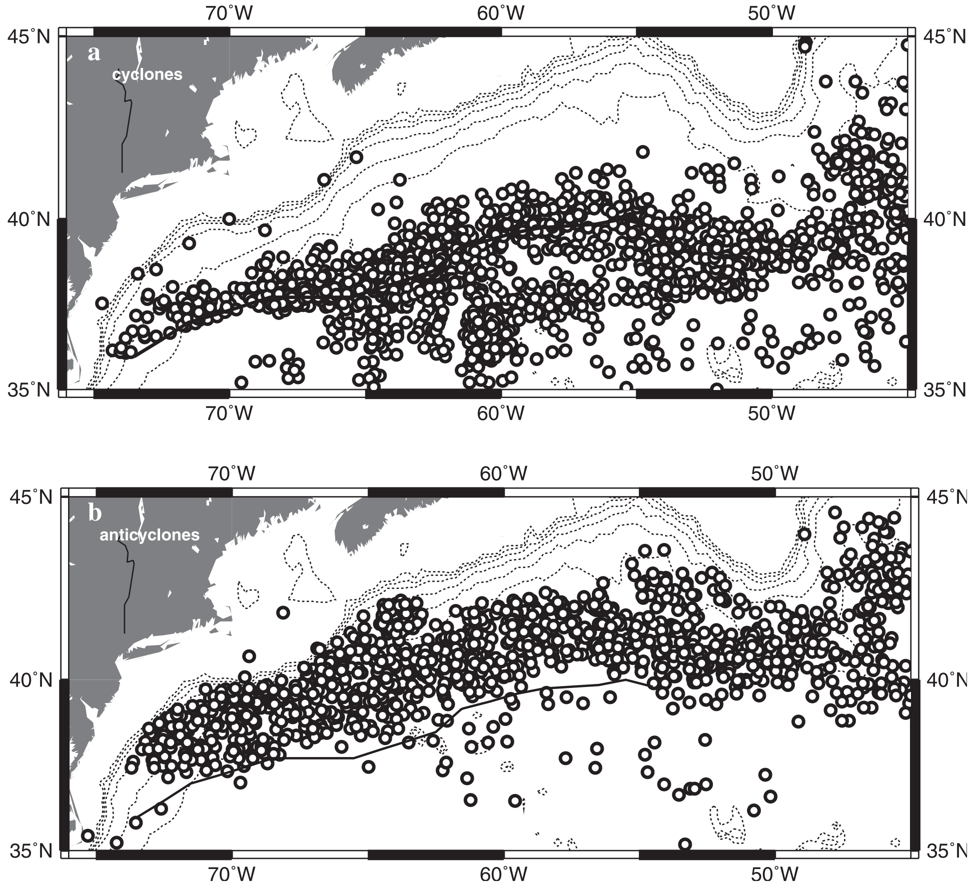

Figure 4. Daily positions of cyclonic and anticyclonic features with velocities larger than 0.5 m s^{-1} (after filtering the velocity time series with a 2 day Lanczos filter). A feature is selected when the directions of acceleration and velocity differ by at least 45° and when the component of acceleration orthogonal to velocity is at least 5% of the Coriolis force.

systems. This spatial distribution is found in earlier maps with coarser resolution [*Richardson*, 1983; *Brügge*, 1995; *Rossby*, 1996] (*Rossby* [1996] being based on a subset of the data used here). In the midbasins, local maxima of EKE in excess of 250 cm^{-2} s^{-2} are found in the branches of the NAC and the AC, as depicted in analyses of altimetric data [*White and Heywood*, 1995; *Ducet et al.*, 2000]. In the subpolar gyre north of 55°N the northward branches are associated with maxima in EKE, in particular, to the northwest of the Maury Channel (20°–25°W), where there is a large number of trajectories with velocities larger than 50 cm s^{-1}. There is also a local EKE maximum off west Greenland in the eastern Labrador Sea (60°–62°N). The spatial structure of EKE is very similar to estimates of geostrophic EKE from altimetry for 4 years (between 1987 and 1994) preceding most of the drifter data [*White and Heywood*, 1995] and also during 1993–1999 [*Ducet et al.*, 2000].

[23] Between 40° and 50°N, EKE usually increases from east to west until reaching the NAC or GS. There is a decrease farther west both in the Mid-Atlantic Bight and the shelf areas off North America, as well as west of the NAC. North of 43°N, there is often a weaker maximum near the shelf break associated with the Labrador Current. There is a sharp decrease south of 33°N south of the GS and the AC. In the western Atlantic the weakest EKE is found near 30°–32°N, but at this latitude, EKE is much weaker farther east between 22° and 40°W (50 cm^{-2} s^{-2}). Similarly, low EKE values are also found between 36° and 43°N in the eastern Atlantic, as well as southwest of Iceland. Low EKE levels are further found in the southern part of the Labrador Sea as well as just north of the Subpolar Front near 53°N (30°–40°W).

[24] The trajectories with velocities larger than 1 m s^{-1} are mostly found in the vicinity of the GS and NAC west of 37°W (Figure 3). The trajectories in the GS east of 65°W are usually strongly curved, indicating the presence of meanders or eddies. They are also curved in the NAC, but the meanders and eddies appear there quite repetitively at the same position. There are also large velocities in the Florida Current near the shelf break or in the GS west of 65°W and in the east Greenland Current close to the shore south of 65°N. These trajectories have much less curvature and follow the bathymetry.

[25] The velocities between 0.5 and 1 m s^{-1} also show the NAC and GS but over a broader band. For the GS this band is sharply delimited to the north by curved trajectories that are often anticyclonic (Figure 4). West of 65°W, they are often detached from the GS (warm-core rings [*Olson*, 1980; *Richardson*, 1983]), but east of 65°W they often remain attached (meanders, as seen by the alternation of cyclonic and anticylonic curvature along the trajectories). South of the GS, there is a more frequent occurrence of cyclonic trajectories, all the way east to 45°W. These latter

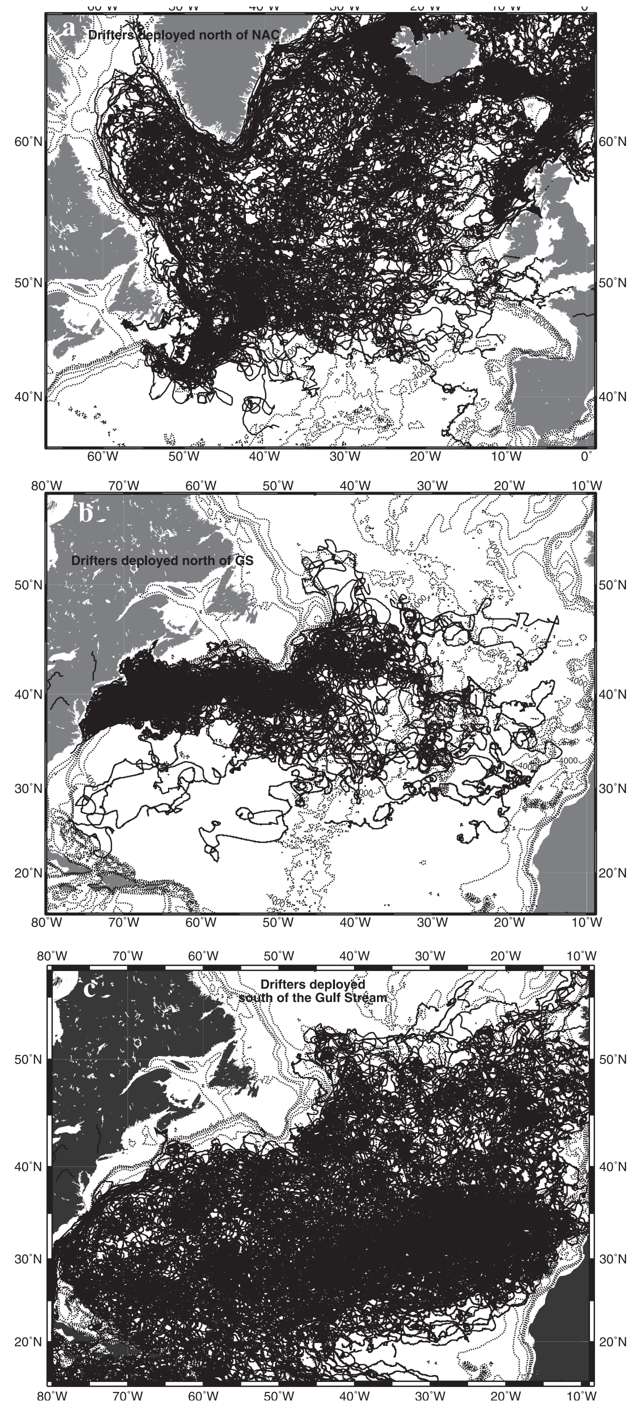

Figure 5. Trajectories for different areas of launching: (top) for the Labrador Current and subpolar gyre north of 52°N, (center) for the area north of the GS and west of 50°W, and (bottom) for the subtropical gyre and areas south of 50°N.

also correspond to meanders of the GS or separated cyclonic cold-core eddies.

[26] The western edge of the region with large buoy drifts in the NAC is also very clearly defined (Figure 3) and separates quite well from a vein of large velocities in the Labrador Current near the shelf break. Southeast of the GS, the area of large currents extends into the AC near 33°–34°N. North of 50°N, trajectories with large velocities extend into the eastern subpolar gyre, in particular, in the areas of large EKE, which correspond to the different branches of the NAC that flow into the subpolar gyre interior. Interestingly, these trajectories are not often in the direction of the average current, which is compatible with a high ratio of eddy to mean kinetic energy (not shown). Large velocities are also found close to southeast Iceland,

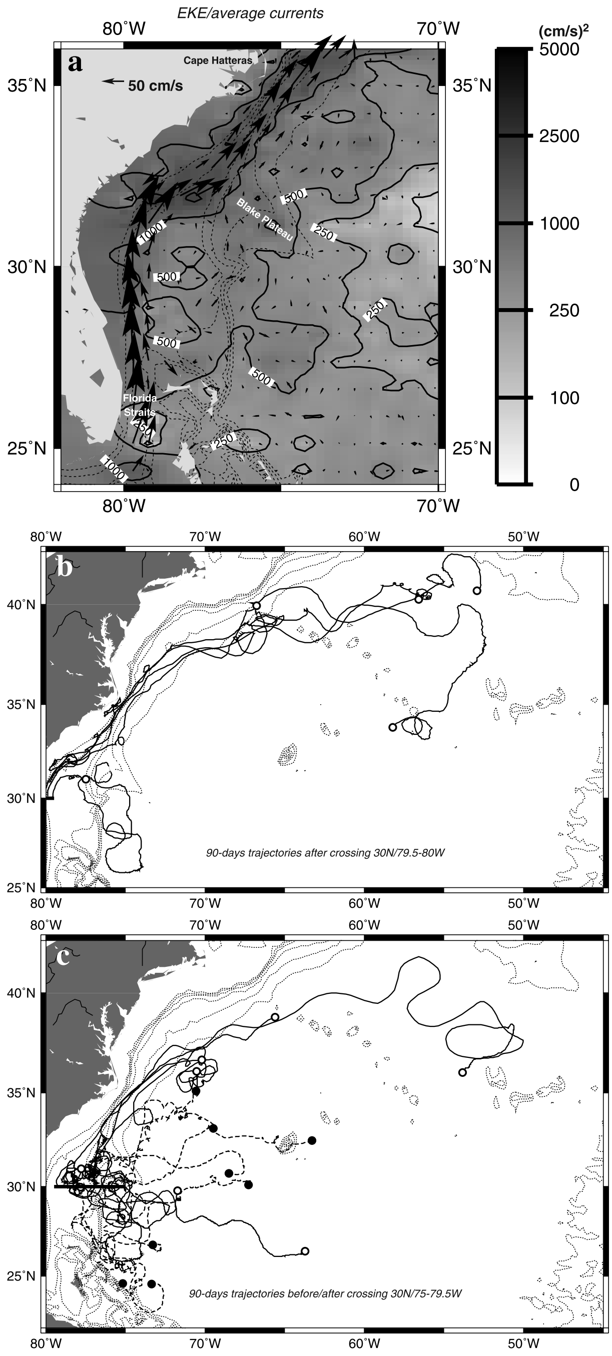

Figure 6. The Florida Current region: (a) average current and EKE in the Florida Current (with an increased zonal resolution of 0.5°) and (b) and (c) 90 day trajectories before (dashed line) and after (solid line) crossing 30°N for two different longitude ranges (shaded (open) dots at beginning (end) of trajectories).

the Iceland-Faroe Ridge, the southern Norwegian Current along the shelf break, and the east (both shore and shelf break branches) and west Greenland Currents. There are also some energetic features in the interior of the Labrador Sea between 60° and 62°N.

[27] Surface water displacements can be followed by viewing a selection of trajectories of drogued drifters that were deployed in specific areas. These trajectories are of variable duration, with few exceeding 1 year. Three areas of deployment are selected (Figure 5): north of the Gulf Stream (representing slope water), in the subpolar gyre including the Labrador Current and all areas north of 51°N, and deployments elsewhere. In the western Atlantic, trajectories from these areas of deployments remain bounded most effectively by the Gulf Stream system, especially west of 55°W (only four floats crossed it, three from the north and one from the south). Trajectories from the three domains become intertwined in the North Atlantic Current north of 42°N in the western Atlantic, although a large share of the trajectories reaching 47°N have been deployed either in this region or in the cold waters of the Labrador Current.

4. Regional Circulation

[28] We will use trajectories of 15 m drogued drifters to illustrate regional patterns. We are interested to see how they differ from the average circulation depicted in the Eulerian averages, having in mind to learn where particles reaching a particular well-defined Eulerian current originate and where they subsequently go. The deployment strategy has a stronger influence on where the particles come from than on where they end up, so caution has to be applied in interpreting this information.

[29] The regional description will start with the Florida Current followed by the GS and the recirculation pattern to the south and the extension of the subpolar gyre to the north. Next, we will discuss the midbasin current systems, the AC, the NAC and Labrador Current east of the Grand Bank, and the various branches of the NAC across the Atlantic. This is followed by a discourse on the interaction of the warm portion of the NAC circulation with the subpolar gyre and the Nordic Seas and concluded with the circulation around the Irminger and Labrador Seas.

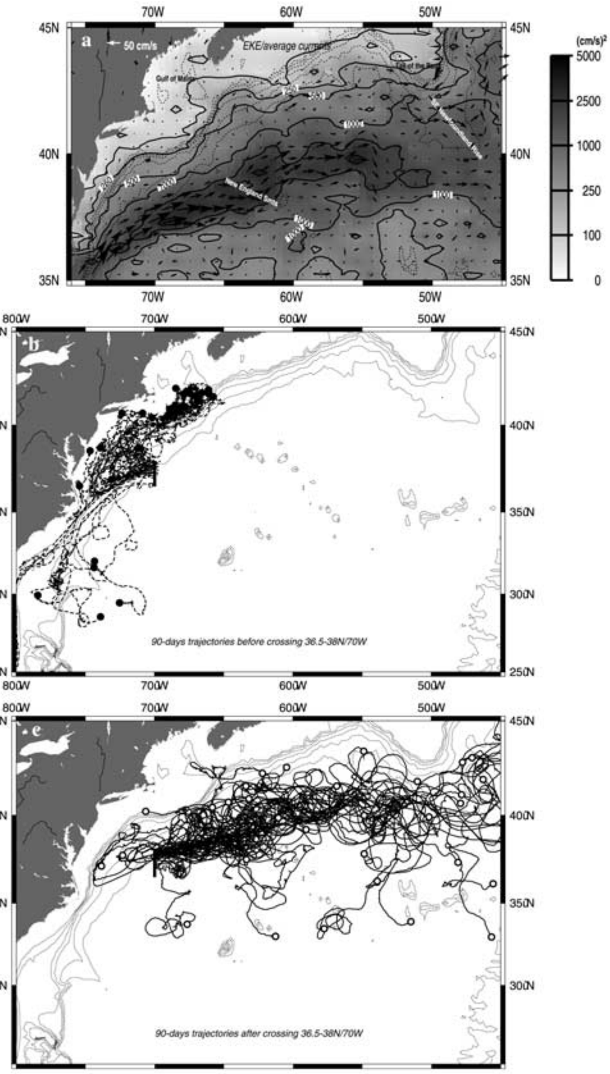

Figure 7. The Gulf Stream region: (a) average current and EKE (weight given to drifters deployed north of GS is 10% of weight for other drifter data) and 90 day trajectories (b) before (dashed line) and (c) after (solid line) crossing the Gulf Stream at 70°W (shaded (open) dots at beginning (end) of trajectories).

4.1. Florida Current

[30] Both the average Eulerian Current (Figure 6a) and trajectories with high velocity (Figure 3) depict a Florida Current continuous from the Florida Straits to Cape Hatteras. The high-velocity drifters travel close to the continental margin with an eastern boundary that is associated roughly with the 500 m depth contour north of the Blake Plateau and Ridge. North of 32.5°N, the current core with speeds larger than 100 m s^{-1} moves progressively to deeper water and widens to more than 100 km. EKE also strongly increases north of 32°N (the averaging grid on Figure 3 is 0.5° in longitude to increase resolution). Out of eight trajectories that crossed 30°N (Figure 6b), six continued eastward in the GS, three of which reached a longitude east of 55°W within 90 days. Two drifters that were on the offshore side of the Florida Current at 30°N veered offshore before they reached Cape Hatteras.

[31] East of the Florida Current axis, the Eulerian velocity decreases and reverses to a weak southward current at 79°W south of 31°N. Several drifters move counter to the Florida Current very close to its eastward flank (Figure 6c). Farther eastward, over an ocean depth larger than 1000 m, north of 27°N, there is evidence of another vein of northward current centered at 77°W with weaker average velocities than the Florida Current, although often exceeding 50 cm s^{-1} on individual trajectories (Figure 3). Most of the trajectories in this current vein originate from the subtropical gyre mostly directly to the east (this flow from the interior is expected from theory, as reviewed by *Schmitz and McCartney* [1993]). Out of seven drifters in this northward flowing vein, three eventually entered the GS a short distance upstream of Cape Hatteras. Two drifted to the east-southeast roughly in the subtropical convergence of the western North Atlantic near 28°N [*Leetmaa et al.*, 1977; *Pollard and*

Regier, 1992]. North of 27.5°N, the average current farther offshore has a southward component indicating some recirculation (two drifters went from the latitude of Cape Hatteras to 30°N with some indication of cyclonic looping).

4.2. Gulf Stream

[32] Near Cape Hatteras, numerous drifters entered the GS from deployments farther north, in particular, from deployments made in the Mid-Atlantic Bight and George Bank [*Lozier and Gawarkiewicz*, 2001]. These drifters (Figure 7b) usually veer northeastward northeast of Cape Hatteras. Upon being entrained in the GS they accelerate quickly by up to 1 m s^{-1} in a day, which implies a large deviation from the geostrophic balance. However, they travel eastward parallel to the north wall of the Gulf Stream until at least 65°W with a velocity that is often less than the ones of drifters arriving from the Florida Current. To minimize the biases related to the uneven number of drifters arriving from the north compared to those arriving from the south, we have reduced by a factor 10 the weight of data from drifters deployed north of the GS (this homogenizes the data density and minimizes the array bias) to composite a Eulerian mean (Figure 7a). This average current differs very little from the one presented on Figure 2 and displays a stronger GS near Cape Hatteras and a more zonal GS west of the New England Seamounts (see comparison in Appendix A).

[33] Near Cape Hatteras the average GS is portrayed as a current toward the northeast, which quickly veers eastward with an anticyclonic turn. It then undulates in numerous meanders while remaining clearly identifiable as a strong velocity core until 55°W, 40°N. The position of the core of the strong average current (Figure 7a) is at all longitudes within 100 km north-south of the average one depicted in frontal analysis from advanced very high resolution radiometer (AVHRR) data [*Lee and Cornillon*, 1995], altimetric data [*Kelly*, 1991] or the "Oleander" acoustic Doppler current profiler (ADCP) data at 70.5°W, 37.2°N [*Rossby and Gottlieb*, 1998]. The ADCP data correspond more closely to the time period of the drifter data with the position from the drifters a little to the north (0.2°) to the one in the ADCP data. The width of the average GS from Figure 7 is also consistent with the ADCP data, which indicate that the average Eulerian GS extends over a little more than 1° of latitude. The maximum amplitude of 1.1 m s^{-1} depicted in the averaged ADCP data is significantly larger than the velocity indicated in the closest 0.5° × 1° bin (0.85 m s^{-1}) and is an artifact of the different scales used in either treatment.

[34] Both this analysis and the ADCP data [*Rossby and Gottlieb*, 1998] portray extensive westward recirculations at 70°W centered 1.5°–2° both north and south of the Gulf Stream core. The position and intensity of the recirculation experienced large year-to-year fluctuations in the ADCP data, which is also suggested in altimetric data but could not be described with the limited data set of drifters south of the GS.

[35] The map of the mean current (Figure 7a) suggests a deceleration of the GS and a northward shift in the vicinity of the New England Seamounts near 63°W, 38°N. The area of the New England Seamounts is bifurcated by high-velocity trajectories that expand meridionally to the east. Numerous

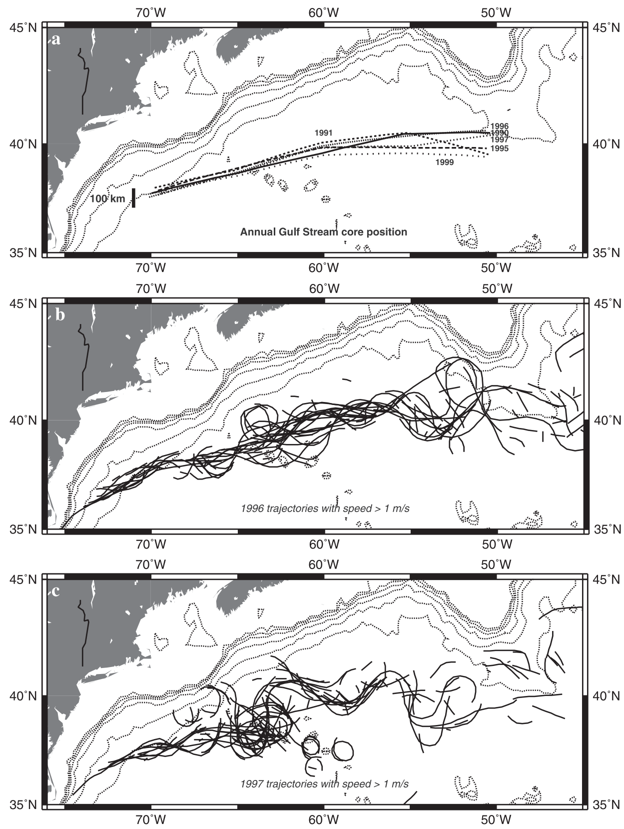

Figure 8. Core velocity of the Gulf Stream: (a) median position of the high-velocity trajectories estimated at different longitudes for the different years sampled by drifters and high-velocity trajectories in the Gulf Stream area for the years (b) 1996 and (c) 1997.

loops or nonstationary meanders can be detected to the east of the seamounts (Figures 7c and 8). This area is associated with a maximum EKE extending to 61°W over a 2.5° latitudinal band. This more extensive drifter data set does not show the southeastward extension of high EKE found by *Richardson* [1983] from a more limited data set. This northward shift of the current axis is not that clear in other data sets of positions of the Gulf Stream, although hints of it can be found in both Richardson's drifters and in the AVHRR north wall average position. It is not found at all in *Kelly*'s [1991] analysis of the Geosat altimetric data. Because this feature disappears when the current drifter data are grouped in specific years, it is not very robust and could well be a feature of the particular years sampled by these drifters.

[36] To get a sense of the changes of position of the GS, we examine more specifically the trajectories presenting a velocity larger than 1 m s^{-1}. ADCP measurements near 70°W indicate that the instantaneous width of the part of the GS with velocity larger than 1 m s^{-1} averages 60 km near 70°W [*Rossby and Gotlieb*, 1998]. *Rossby* [1999] indicates that this is nearly independent of longitude or of the presence of meanders, at least west of 55°W. The region where speeds larger than 1 m s^{-1} are found (Figures 3, 8b, and 8c) expands after leaving Cape Hatteras. Drifter data with large speed present small-amplitude meanders at least until 65°W, and perhaps to 63°W, where the GS crosses the

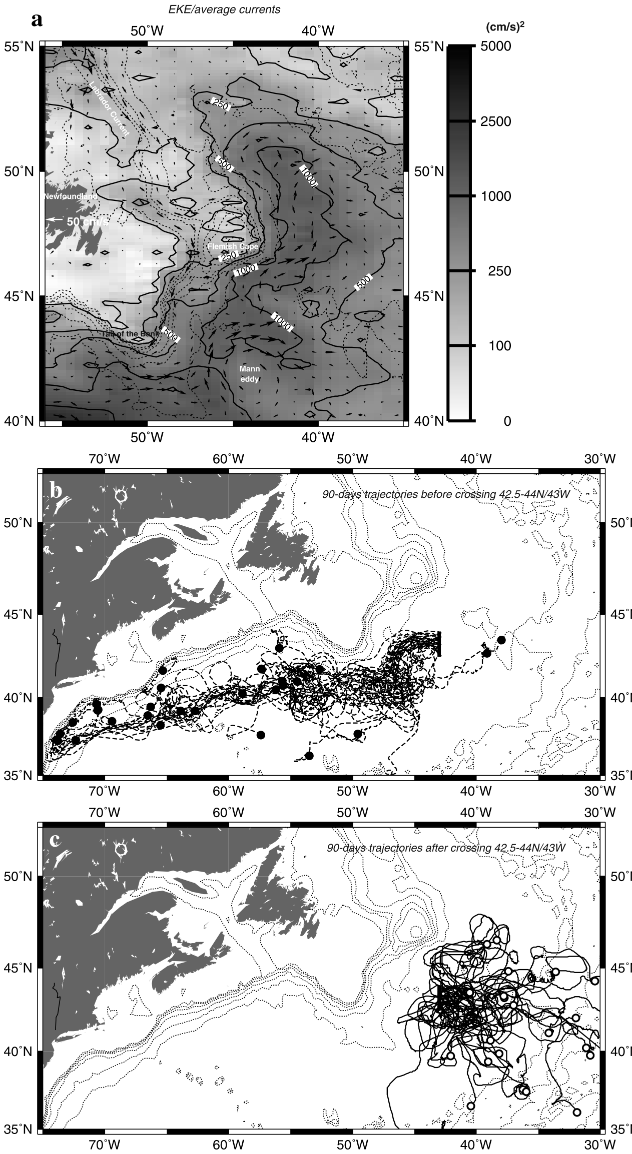

Figure 9. The NAC region east of the Grand Bank: (a) average current and EKE (200, 500, 1000, 2000, 3000, and 4000 m isobaths) and 90 day trajectories (b) before and (c) after crossing the north flank of the Mann eddy, (d) and (e) 44°N between 43° and 45°W, and (f) and (g) 44°N between 45° and 48°W (same as Figures 7b and 7c).

New England Seamount chain. At 72°–65°W the width of this high-velocity core is on the order of 150 km. Therefore the spread of the trajectories with large velocities much larger than the instantaneous GS is indicative of the variability of the GS path and of its associated eddy field. This spread was already noticeable with the few earlier drifters presented by *Richardson* [1983].

[37] Various authors have discussed the changes in GS position that happen on seasonal to decadal timescales and are particularly easy to notice in the western part of the path [e.g., *Kelly*, 1991; *Lee and Cornillon*, 1995; *Rossby and Gottlieb*, 1998; *Joyce et al.*, 2000]. *Rossby and Gottlieb* [1998] comment on displacements from the mean path that can at 70°W exceed 50 km in the meridional direction. For the period sampled by the drifters they find a more northward position of the GS core in 1995 than before or after 1997. These changes appear to be confirmed by analyses of altimetric data by *Frankignoul et al.* [2001].

[38] The number of SVP trajectories is not sufficient to resolve short-period fluctuations, for example, the dominant period at 9 months shown by *Lee and Cornillon* [1995]. As an indication of the time variability, trajectories corresponding to a velocity >1 m s^{-1} are grouped by year. Only 1990, 1991, 1995, 1996, 1997, and 1999 have enough trajectories. The 1997 composite (Figure 8c) corresponds to a particularly pronounced northward shift near the NE seamounts (1990 to a lesser extent) and was associated with very large meanders with considerable variability in their position. On the other hand, 1995 and 1996 showed no clear northward shift and less meandering (Figure 8b). The average position of the GS core is estimated by taking the baricenter of the positions with high velocities within a 5° longitude window (Figure 8a). It indicates relatively little interannual variability in the position of the GS during these years, in line with what *Rossby and Gottlieb* [1998] find at 70°W. Interannual variability is larger farther east. Results from satellite altimetry presented by *Frankignoul et al.* [2001] or *Ducet and Le Traon* [2001] do not corroborate the year-to-year changes obtained here from the drifters. This is not surprising because of an insufficient sampling of the variability by the drifters [see also, *Fratantoni*, 2001]. Also, drifters were mostly drifting from deployments to the north of the GS in the early years, which probably contributes to a more northerly position in the composites than for the later years (1997 and 1999) when drifters began to transit through the GS from the Florida Current.

[39] Between 61° and 55°W the average flow appears more zonal. At 55°W, there is a significant weakening of the average flow (EKE remains large), and the first branching of the GS occurs. One part continues a little to the north to 41°–42°N, and a second branch continues to the southeast (38°–39°N) around a topographic trough centered near 53°W. This branching is not described as such in earlier work, but we have already seen it in the average velocity maps. The northern branch has been usually identified with a slope current, and the southern one with the GS. The northern branch has less EKE than the southern branch, and in it, there are no trajectories with velocity >1 m s^{-1} (notice, however, that the average velocity in the northern branch is larger than in the southern branch, so that the difference in EKE suggests more topographic control, as well as a weaker jet for the northern branch). We will continue to describe these branches in the Eulerian composite after a further discussion of the behavior of the trajectories within 90 days of travel on either side of specific sections across the GS (Figures 7c and 9).

[40] Several trajectories that cross 70°W in the GS are found within 90 days in the northern branch, although a larger number of trajectories in the GS at 70°W cross 50°W farther south (Figures 7c and 9). In addition to drifters originating from the GS, the northern branch is also fed by trajectories originating from an area more closely associated with the Slope Water Current. The Slope Water Current flows at the 4000 m isobath from at least 63°W and roughly corresponds in this western part to the northern limit of high

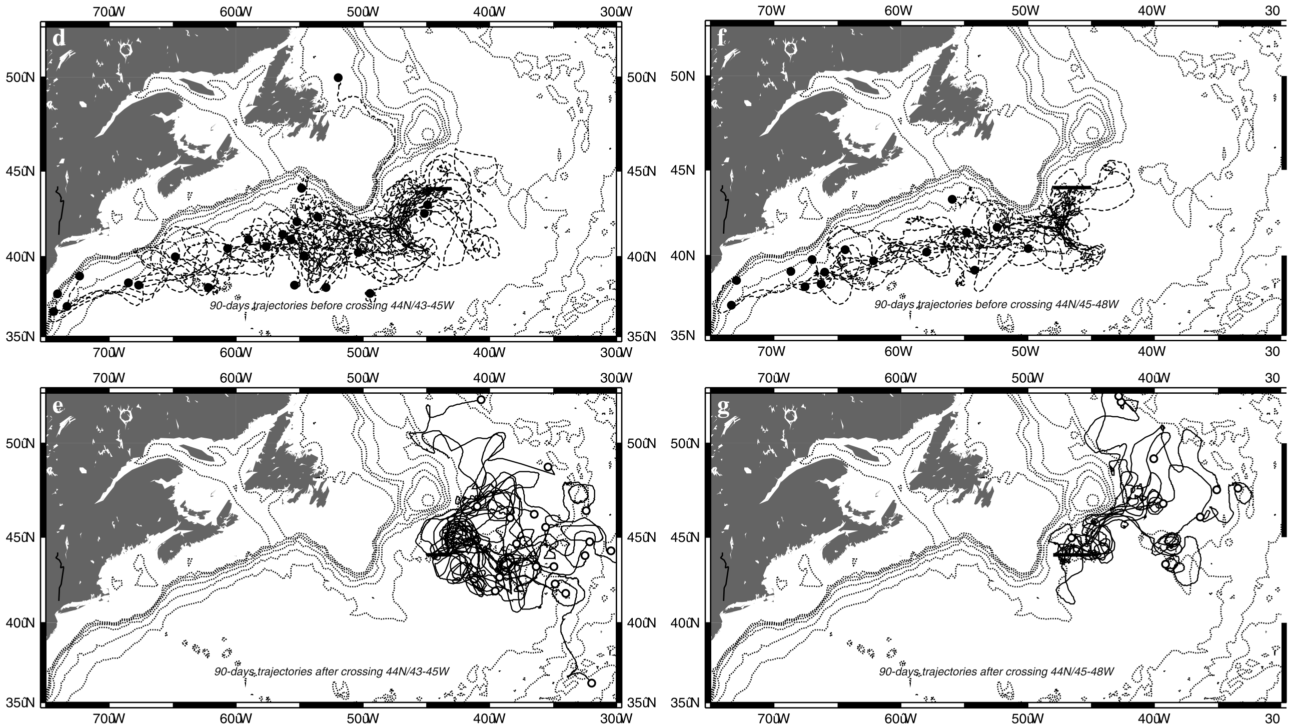

Figure 9. (continued)

EKE and of the looping trajectories. A few trajectories follow the 4000 m isobath eastward, although never the whole stretch from 63° to 50°W (a few on Figures 7c, 9d, and 9f). These often correspond to the northern part of anticyclonic meanders of the GS (Figure 4) with trajectories ending often at much lower latitudes. In general, the distinction in individual drifter tracks between the two branches of the Gulf Stream is only valid for a short zonal stretch, suggesting vigorous mixing between the branches indicated by the mean Eulerian velocity map.

[41] Near 50°W, just west of the tail of the bank, the northern branch now merges with a current that carries drifters originating from the Labrador Current system. This merged eastward current centered near 41°N at 50°W, where it crosses the southeast Newfoundland rise, has some distinctive characteristics not found in the Slope Water Current farther west. It is more intense and is fed by both the Gulf Stream and the Labrador Current, and its EKE increases significantly. Hydrographic observations that cover many decades [*Mann*, 1967; *Pickart et al.*, 1999] reveal a similar average position of the strong eastward current vein we see in the drifters and a distinction in the water mass properties from the Slope Water Current.

[42] The southern branch of the GS, where the highest drift velocities are usually found (Figure 3), is present in all seasons but is not well delineated in data divided into specific years. In this region many drifters travel southward out of the area of highest EKE. The southern branch, south of 40°N, is also a region of high EKE (Figure 2) that rapidly decreases east of 54°W. Individual trajectories show a wide variety of paths, as was also indicated in the smaller data sets presented by *Richardson* [1983], *Krauss et al.* [1990], and *Käse and Krauss* [1996]. Interestingly, at 54°W, there is also a southward bend in the position of the maximum velocity variance from TOPEX/Poseidon and ERS satellite altimetric sea level slope observations [*Ducet et al.*, 2000].

4.3. Azores Current

[43] The southern branch in all seasons crosses the Newfoundland rise near 38.5°N and extends eastward at least until 42°W. Surprisingly, according to the drifters most of the southern branch of the GS flows southward and westward in a recirculation pattern rather than feeding the NAC, the Mann eddy, or the AC. The region where the recirculation is initiated is highly variable in time and not defined at the same place for yearly subsets of the data. A small region east of 55°W and north of 35°N displays a westward Eulerian current with velocities of about 10 cm s^{-1} (Figures 2 and 7a). Farther west, the recirculation pattern is not well determined as a coherent current but rather as a broad, eddy-filled drift to the west.

[44] A few of the trajectories from the southern branch of the Gulf Stream reach a band of average eastward flow that is evident at 55°W and more clearly at 45°W. This band extends from 34°–34.5°N at 45°W to the African continental rise at 33.5°–34°N and is usually referred to as the AC (Figure 2). Also, a few drifters originating from the anticyclonic Mann eddy centered near 44°W, 42°N reach the AC (Figure 9c), and their path is somewhat different from what was diagnosed from analysis of drifters with drogues at 150 m by *Krauss et al.* [1990]. However the connection of the AC with the GS is not strong in this data set, as most of the drifters in the AC at 30°W were not in the GS or the NAC within the past 6 months. This could be due to the fact that a large number of drifters were deployed in

the Azores region [*Zhou et al.*, 2000] and virtually none were deployed near 40°–60°W farther west.

[45] As discussed by *Reverdin and Hernandez* [2001] and *Zhou et al.* [2000], drifters do not stay in the AC system for more than 2 months. Most leave before the current turns southward in the region of the Madeira plateau. The mean flow on either side of the AC is very slow, which results in fairly slow eastward displacements of the drifters. For example, in 3 months, none of the drifters initially in the AC at 30°W had reached 20°W, and the average eastward displacement was 4° (an average zonal velocity of 3.8 cm s^{-1}). The eastward average AC is associated with larger EKE than to its north or south, which is most noticeable east of the MAR at 36°W (Figure 2). *Zhou et al.* [2000], using a large subset of the drogued data used here, note that EKE within the AC is largest on its southern flank.

[46] A large number of the drifters in the AC are entrained in the subtropical gyre circulation, quite commonly east of Madeira (17°W) where many trajectories veer southwestward. EKE levels are very low between 23° and 40°W in the subtropical gyre south of the AC.

4.4. North Atlantic Current

[47] Most of the drifters that arrive in the area north of Newfoundland Rise do so in the northern branch of the GS after crossing the rise near 41.5°N. Many trajectories move to the southeast parallel to the northern flank of this 3000 m deep ridge and then turn back to the north, again following closely the ridge morphology before ending up in a large anticyclonic feature (Figures 7 and 9). This circulation pattern is consistent with the presence of a cold wedge seen often on the March AVHRR imagery [*Rossby*, 1999]. This wedge separates the GS from a large anticyclonic semi-permanent Mann eddy to its north, centered near 44°W, 42°N [*Mann*, 1967]. This wedge is often present on individual ship surveys, as, for example, *Clarke et al.* [1980], who find it in April–June 1982, *Krauss et al.* [1990], who find it in March–April 1987, and *Caniaux et al.* [2001], who find it in early 1997. The drifter data show that the surface water masses follow the subsurface circulation pattern that has been extensively discussed from water masses and circulation observations with a variety of techniques [*Schmitz and McCartney*, 1993; *Käse and Krauss*, 1996; *Rossby*, 1996].

[48] The Mann eddy is well defined in the average current map (Figures 2, 9, and 8a) and in the high-velocity trajectories (Figure 3). Its presence is supported by the analysis of subsets of the data and is also present in drifter trajectories drogued to 150 m [*Käse and Krauss*, 1996], as well as in hydrographic analyses from different periods [*Kearns*, 1996]. The 1 m s^{-1} trajectory segments are found mostly on its western and northern flanks. Two thirds of the trajectories that cross its western and northern flanks (Figure 9b) arrive from the GS, and the stability of their paths indicates that the western and northern portions of the Mann eddy are quite stationary or perhaps convergent at the surface. Several drifters complete an anticyclonic loop several times, and because this is not a regular occurrence, its eastern limb might be more variable or in fact divergent at the surface. The looping at the surface is much less noticeable than on some subsurface floats presented by *Rossby* [1996], suggesting wind effects on the surface layer. Within 3 months travel time the surface drifters have experienced a wide meridional spreading, more to the south than to the north. Only one has reached the AC, and 4 out of 16 having reached the MAR.

[49] The trajectories north of 44°N to the north and northwest of the Mann eddy become progressively less regular. Some of the drifters that pass through the two sections of the NAC on Figures 9d and 9f originate through the northern side of the Southeast Newfoundland Rise, but the majority are derived from the GS. In the area 45°–48°W, which intersects the 4000 m isobath, 4 out of 19 drifters have passed through the Labrador Current in the past 90 days. The trajectories now follow rather closely the path of the average NAC illustrated in Figure 2, which translates them to 50°N, where a drift to the east begins. It is quite remarkable that none of these drifters crossed the Subarctic Front to its cold and fresh sector west of the MAR, whereas a few Rafos floats crossed it.

[50] Drifters that crossed 44°N east of 45°W experience a wider variety of trajectories in a large fan that spreads eastward and southward of 50°N. The barycenter of gravity of these remain close to 45°N, even though one drifter reached the vicinity of the AC. We note that an anticyclonic structure centered near 42°W, 45°N (Figure 9e) appears in their tracks. This feature was also well identified by subsurface float trajectories [*Rossby*, 1996] and described by a hydrographic survey [*Caniaux et al.*, 2001], as well as by the average geostrophic circulation [*Kearns*, 1996]. This feature is not identified as a closed circulation on the average current maps (Figure 2), which suggests some variability in its position. Large average currents are found near its northern flank southeast of Flemish Cap.

[51] It is apparent from a variety of observations, including the drifter data, that there exists a series of quasi-stationary cyclonic and anticyclonic features in the NAC [*Krauss et al.*, 1990; *Kearns and Rossby*, 1998; *Carr and Rossby*, 2001]. With both mean current maps and individual drifters the anticyclonic features are better defined (42°W, 45°N; 39°W, 46.5°N; 40°W, 49°N; and 43°W, 50.5°N) than the cyclonic ones, whereas the subsurface floats identify both [*Rossby*, 1996]. In the drifter data the western boundary of the quasi-permanent eddy circulations and NAC correspond roughly to the 4000 m isobath. Transient NAC eddies are found up to 53°N following the 4000 m isobath extensions to the north and west that were also described by *Lazier* [1994], but they occur in a region with only a weak average current.

[52] In the NAC, highest EKE is closely associated with the regions of large speed (1 m s^{-1}) trajectories and with strong mean currents, in particular, north of the Mann eddy near 44°N and near 47°–49°N in the area where the NAC turns northward. The envelope of the trajectories with velocities larger than 0.5 m s^{-1} clearly delineates the western boundary of the circulation associated with the NAC (Figure 3). It extends a little bit westward of the average current, although it clearly follows its path. However, in general, the large EKE field, in excess of 300 (cm $s^{-1})^2$ spreads farther to the east and south from the NAC and the GS systems than it does to the north.

[53] The NAC gains fluid from the Labrador Current at different latitudes, in particular, near 44.5°N south of the

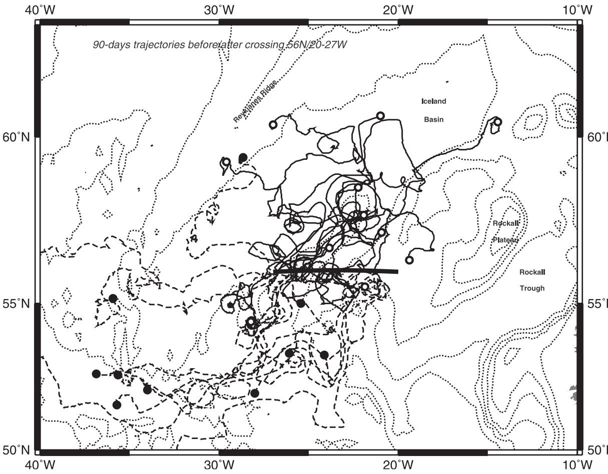

Figure 10. Ninety day trajectories before and after crossing the Maury Channel at 56°N (same as Figure 6c).

Flemish Pass, where a branch with large velocities can be traced westward to the Labrador Current, and near the tail of the bank near 43°N. An important branch of the Labrador Current is intensified in an anticyclonic sense around the shallows of the Flemish Cap (centered near 45°W, 46°N) before joining the Subarctic Front along the NAC east of the Cap. The NAC looses fluid to its east, in particular, at the latitudes of the eastward branches and, more specifically, near 43°–44°N and north of 47°N.

[54] The region to the southeast of the NAC main current system is quite variable as different subsets of the data set indicate different structures of the eastward drift. Both individual tracks as well as the average current field present no more clear a picture than hydrographic surveys [e.g., *Sy et al.*, 1992; *Caniaux et al.*, 2001] or data from drifters drogued to 150 m [*Krauss and Käse*, 1984; *Krauss et al.*, 1990]. On a very large scale, of, say, 500 km the average flow north of 40°N is eastward east of the energetic EKE region of the NAC and extends to a boundary located between 40°N, 35°W and 45°N, 8°W. South of that line, which is associated with a sharp decrease of the winter mixed layer depth in different climatological data sets [*Lamb*, 1984], the average flow becomes even weaker and develops a southward component.

[55] North of 48°N, the Eulerian flow continues to show a high degree of organization (Figure 2). Two separate branches of average eastward current are identified at 50° and again at 52°N, which appear to correspond to the average positions of the North and South Subartic Fronts according to hydrographic surveys [*Belkin and Levitus*, 1996]. Individual trajectories remain within a particular branch only west of 32°W, whereas farther east, the separation is less clear. The drifters in the southern branch (50°N), which has higher EKE, have larger meridional excursions, probably associated with meanders of the Subarctic Front. The 11 drifters in the northern branch travel to the Icelandic basin east of the MAR, whereas drifters in the southern branch have a wider spread with 6 having crossed 35°W drifting farther south and 13 heading farther north. The two current branches were also observed with subsurface Rafos floats, suggesting an influence of the topography of the MAR with the two main deep fracture zones at these latitudes [*Bower et al.*, 2000].

4.5. Subpolar Gyre

[56] The subpolar gyre has two parts. The eastern segment serves as conduit of the Atlantic water to the Norwegian Sea, and the western part is a gyre with a well-defined cyclonic circulation around its perimeter. In the subpolar gyre, surface currents begin to feel effects of the bottom. The current systems of the eastern part are most complex and are discussed first.

[57] East of 28°W, the average current in the northern branch of the NAC begins to veer northward. This longitude corresponds to the position where the climatological subsurface isotherms that have been trapped west of this region in the Subarctic Front begin to fan out towards the north [e.g., see, *Rossby*, 1999]. Floats at 700 [*Bower et al.*, 2000] and 150 m drogued drifters [*Brügge*, 1995] demonstrate a similar northward veering of the NAC. However, individual trajectories turn to the north at different longitudes, some farther east near 20°W.

[58] The Rockall Trough between Scotland and the Rockall Plateau and the area south of the Rockall Plateau at 20°W receive drifters that originate mostly from latitudes 51°N or lower. Even in the northern portion of the trough near 57°N, only seven drifters originated from the Labrador Current or from the cold waters of the northwest Atlantic north of 51°N compared with five drifters from farther south. Influence of the complex topography of this region is suggested. For example, currents are intensified near 53°N near the 3000 m isobath south of the Rockall Plateau (Figure 2). However, this is also a region of low data numbers and small scales and relative inhomogeneities in EKE that appear in the drifter data but do not appear in the altimetry derived fields [*White and Heywood*, 1995; *Ducet et al.*, 2000]. *Otto and van Aken* [1996] also describe this circulation with a subset of our data. This flow around the Rockall Plateau feeds a strong poleward current along the eastern Atlantic shelf break starting near 55°N. More drifters join it from the west north of Rockall Plateau near 59°N and at the entrance of the Faeroe-Shetland Channel

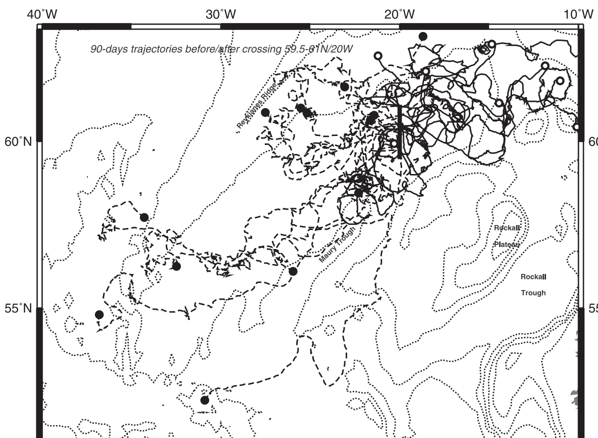

Figure 11. Ninety day trajectories before and after crossing the northern Iceland Basin along 20°W (same as Figure 6c).

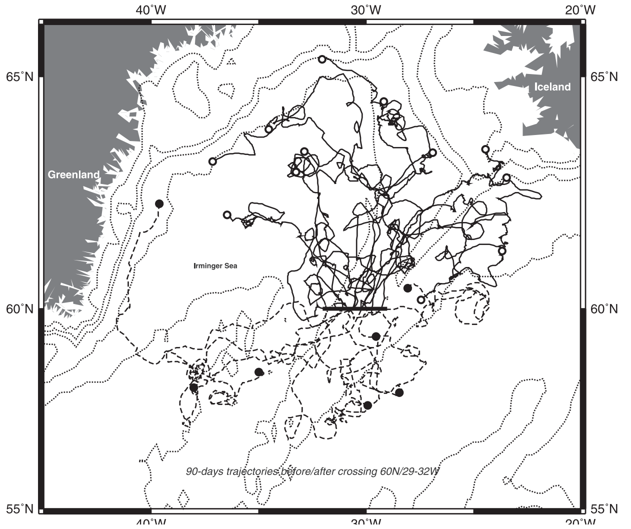

Figure 12. Ninety day trajectories before and after crossing the Irminger Current along 60°N (same as Figure 6c).

near 60.5°N. These are main sources of the Norwegian Current [*Mork and Blindheim*, 2000].

[59] The currents through the Maury Trough, which is the deep channel west of the Rockall Plateau in the Iceland Basin, contains drifters that have mostly passed through the NAC near or north of 52°N (Figure 10). One drifter, however, first moved southward along the eastern flank of the Reykjanes Ridge. Two drifters crossed this ridge from west to east, a feature not found in any subsurface float, nor in the average hydrography, suggesting either transient events or an effect of the wind, possibly because the drifters lost their drogue, which was not correctly reported. After passing through the Maury Trough the drifters continue generally to the north at a low speed so that they are still in the Iceland Basin after 3 months. In the middle of the deep water of the Iceland Basin, drifters move more rapidly (Figure 2) in a fairly narrow vein, reaching 22°W just north of 60°N. The position of this vein does not depend on seasons or on particular subsets of years. The data set there is too sparse to indicate whether its intensity varies from year to year. Using these data and the altimeter composite created by *Ducet et al.* [2000], M. K. Flatau et al. (unpublished data, 2001) compared circulation patterns based on the North Atlantic Oscillation (NAO) index and found significant differences on inter-annual timescales. The northward current system through the middle of the Iceland Basin is intensified with a high NAO index.

[60] Near 60°N, 22°W the average NAC branch of the Maury Trough veers eastward. However, individual trajectories do not suggest a clear continuity with the flow farther south (Figure 11). This area was also crossed by the 100 m drogued drifters deployed close to the Reykjanes Ridge in 1988 [*Krauss*, 1995], which moved mostly in a northeastward direction. Care must be exercised in interpreting the movement of the latter because significant drogue losses occurred that were not monitored by sensors. The eastward movement is sluggish with an average displacement in 3 months corresponding to u = 3.5 cm s^{-1}, but the current system is quickly organized once the drifters flow in a cyclonic fashion around the Faeroe-Shetland Channel. Two preferred paths are either just north of the Faeroe shelf break or flowing along 60°N, a path already known to *Helland-Hansen and Nansen* [1909]. These, together with fluid

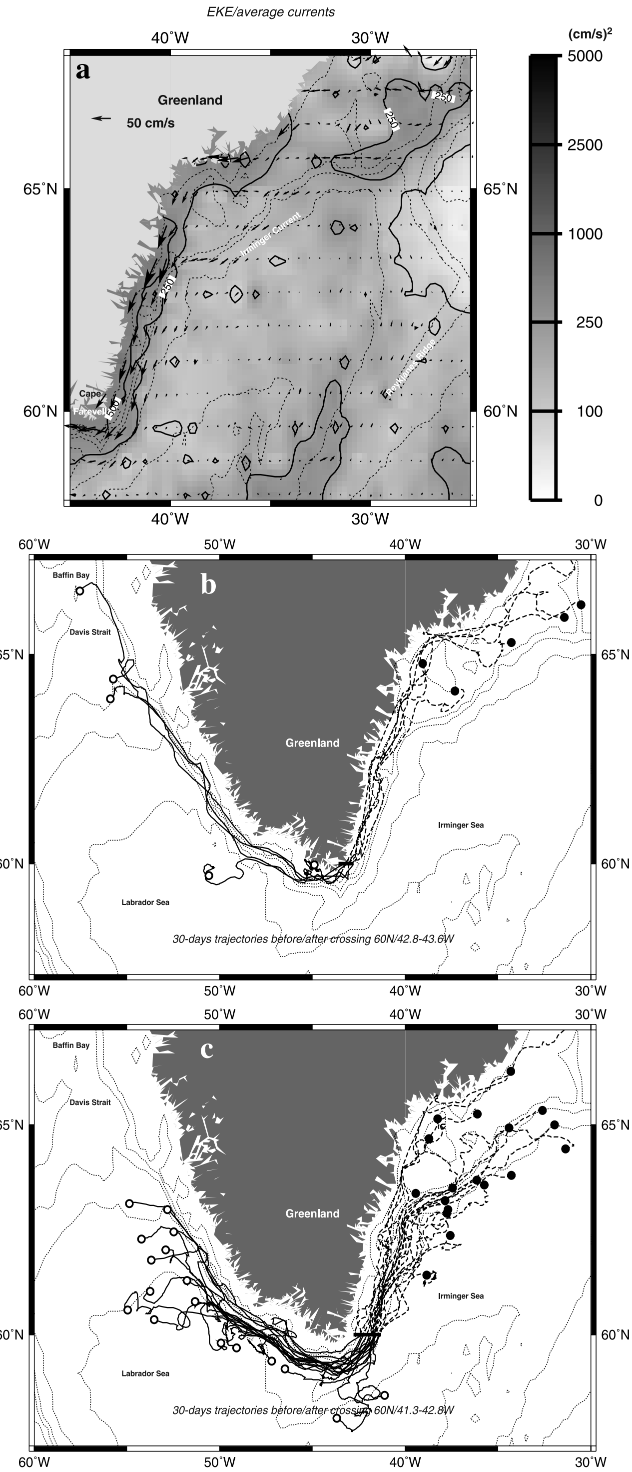

Figure 13. East and West Greenland regions: (a) average current and EKE east of Greenland on a finer zonal grid (0.5°) (200, 500, 1000, 2000, 3000, and 4000 m isobaths) and (b) and (c) 30 day trajectories before and after crossing the East Greenland Current inner branch at 60°N (same as Figure 6c).

originating from the Rockall Trough, feed the shallow branch of the Norwegian Current [*Mork and Blindheim*, 2000; *Orvik et al.*, 2001].

[61] The mean circulation appears weak and not well defined in the Iceland Basin in the approaches of the Iceland-Faeroes Front north until the vicinity of Iceland. The pattern of drifter speeds in excess of 50 cm s^{-1} demonstrates a contiguous jet, yet the mean current is weak. This is because there seems to be seasonal to interannual changes in the circulation that connect flow from the south and east of Iceland to the Faeroes, on the basis of repeated drifter deployments [*Valdimarsson and Malmberg*, 1999]. From the southeast coast of Iceland a portion of the trajectories reach the Norwegian Sea by approaching the Faeroe-Iceland Ridge close to Iceland and then flowing along the Faeroe-Iceland Front. Others cross the ridge farther east near 62.5°–63°N along the shelf break of the Faeroe Islands [*Valdimarsson and Malmberg*, 1999]. These trajectories join the circulation of the Faeroe-Iceland Front, which has been described by *Poulain et al.* [1996] from a subset of this drifter data set. Altogether, the data set contains 20 floats that entered the Norwegian Sea from the Iceland Basin, flowing either north of the Faeroe Islands or between the Faeroe Islands and the Faeroe Bank into the Faeroe Channel.

[62] The western portion of the subpolar gyre is divided by the Reykjanes Ridge with very different characters of flow on its eastern and western flanks. Drifters that ended up on its eastern flank were deployed south of Iceland within its territorial waters. The mean velocity there is not determined by the data set, but on a seasonal to interannual basis, drifters moved southwestward along the eastern flank of this topographic feature (also depicted by *Otto and van Aken* [1996, Figure 1] and earlier 100 m drogued drifters by *Krauss* [1995]). The data suggest that this near-surface circulation is more present in winter than in summer. There is an interesting instance of a trajectory that travels down to 53°N where it joins the flow to the east [see also, *Valdimarsson and Malmberg*, 1999].

[63] Some drifters that initially follow the path to the southwest, cross the Reykjanes Ridge from the Iceland Basin to the Irminger Sea. On the western flank they are joined by drifters from the south (Figure 12) in a poleward current that is a persistent feature on the western flank of the Reykjanes Ridge. This current flows northward from at least 57°N, and associated with it is a local maximum in EKE. A similar circulation was described from 100 m drogued drifters by *Krauss* [1995], although the narrow current along the western flank of the Reykjanes Ridge was not identified. This west flank current is also anticipated from hydrography where a front similar to the Subarctic Front appears and from subsurface floats [*Bersch et al.*, 1999; *Rossby*, 1999; *Lavender et al.*, 2000]. The average flow in the central Irminger Sea is rather weak with a suggestion of a cyclonic circulation with its core near 61°N, 36°W.

4.6. East and West Greenland Currents

[64] The major portion of the flow originating from the western flank of the Reykjanes Ridge flows to the eastern Greenland continental slope along the 1500 m isobath south of the Denmark Strait (Figure 13a). It is called the Irminger Current and is associated with low EKE. It joins the outer

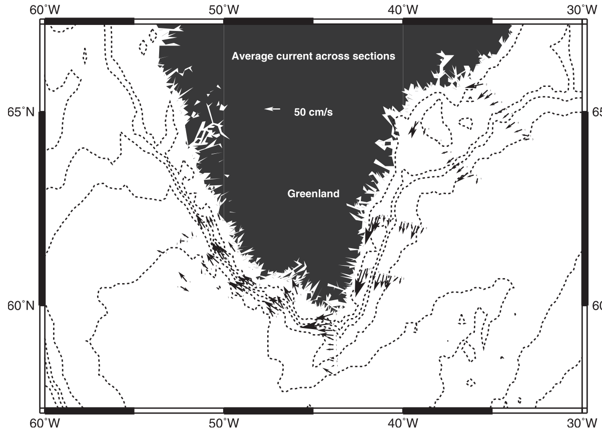

Figure 14. Average current across sections in the East and West Greenland Currents (velocities of drifters having crossed a section are grouped in bins with a resolution of 10–20 km).

branch of the East Greenland Current west of Iceland near 65.5°N, 30°W. A small portion of the flow continues northward on the Icelandic shelf or near its shelf break and veers anticyclonically around Iceland. Offshore of the East Greenland shelf break, the front between the water from the Irminger Current and the water from the East Greenland Current is very sharp and is observed near the surface at least to Cape Farevell. It is associated with a current maximum that is distinct from an inshore branch of the East Greenland Current on the shelf close to the coast near the 200 m isobath and illustrated by the trajectories in Figure 13b. Half the drifters that were in the East Greenland Slope Current at 64.5°N left it before reaching the southern tip of Greenland to drift within the Irminger Sea (not shown). Most of the drifters on the inner shelf are in water of Arctic origin with a strong meltwater influence [*Bacon et al.*, 2002], and stayed in it for nearly 2 months. They all continued past Cape Farewell in the west Greenland Current, three reaching the vicinity of Davis Strait in 1 month and five (out of 7) drifting from the vicinity of Denmark Strait to Cape Farewell in a month. The sampling on the eastern Greenland shelf occurred only in the period when the shelf is ice-free. Topographic features influence the trajectories on the shelf, in particular, the isobaths near 61.5° and 62°N deflect some of the trajectories farther from the coast.

[65] There was only one drifter joining the East Greenland Slope Current at latitudes lower than 63°N, although this happened more frequently in the data set with 100 m drogued drifters [*Krauss*, 1995]. A large proportion of the drifters that were at 63° or at 60°N along the slope (Figure 13), but only half the ones at 64.5°N, were still along the slope farther downstream. These turn in an anticyclonic bend around Greenland following the bathymetry off Cape Farewell to continue as the West Greenland Current. All the drifters drogued at 100 m [*Krauss*, 1995] continued around Cape Farewell and became trapped in the West Greenland Current.

[66] The horizontal structure of the Greenland currents can be investigated further by making several average velocity sections perpendicular to the bathymetry (Figure 14). This indicates that the east Greenland Current maximum velocity

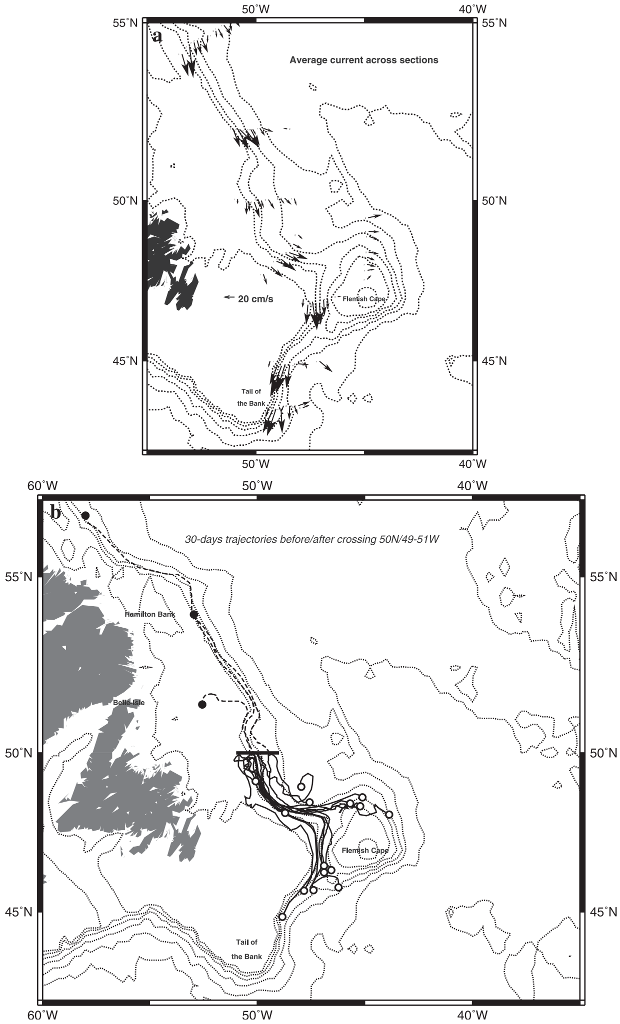

Figure 15. The Labrador Current: (a) average current across sections in the Labrador Current (same as Figure 14) and (b) 30 day trajectories before and after crossing the Labrador Current at 50°N (same as Figure 6c).

on the continental slope is at a water depth between 1000 and 2000 m. We also note a second maximum velocity on the shelf closer to shore. South of Cape Farewell, there is some indication that the inner branch is expelled from the shallower and narrower shelf and is found over water depths of 200–1000 m. Farther along the West Greenland Current, the poleward surface current extends offshore to the 3000 m isobath,and is well identified to at least 64°N. However, all seasons are not equally represented in this analysis, in particular, for the East Greenland Current because of the seasonal presence of ice. There is clear evidence from hydrographic sections done in the spring that the slope current does not always penetrate as far north along the west coast of Greenland [*Buch*, 1984]. The more systematic trapping of the drifters drogued at 100 m might result from the different flow at 15 and 100 m or be related to the small sample size in both cases.

[67] Many drifters were ejected from the West Greenland Current at 60°–62°N, where EKE has a local maximum (Figure 2). It is quite surprising that some looped across the entire Labrador Sea in eddies with decreased speed before accelerating again into the Labrador Current along the western continental slope of the Labrador Sea. Other drifters continued along the slope off Greenland and followed the 1000–2000 m isobath range cyclonically around the northern Labrador Sea. An example of a drifter that circumvented the entire Labrador/Reykjanes Ridge/Greenland circulation system is discussed by *Malmberg and Valdimarsson* [1999]. Three drifters penetrated northward in the Baffin Bay before winter set in. The distribution of drifters in these parts of the Labrador Sea is constrained by the seasonal and interannual presence of ice.

4.7. Labrador Current

[68] There are not many drifters off the Labrador slope north of 55°N. Farther south, there are more data (in particular, summer-autumn), and the sampling of the slope current is adequate to map its structure (Figure 15a), except on the shelf [see also, *Cuny et al.*, 2002]. The maximum current is usually found at depths of 1000 m or less, although it extends offshore to at least 2000 m and probably 3000 m. The current is most intense in the northern part near the Hamilton Bank and presents a minimum near 50°N, a latitude where the continental slope is not as steep. Also, some drifters leave the Labrador Current to the interior of the Labrador Sea, in particular, near 53°N. Caution is required because the seasonal variability suggested by altimetric data and hydrography [*Han and Tang*, 1999] is not adequately resolved here because of the seasonal presence of sea ice. However, this structure is compatible with hydrography (e.g., the diagnostic model of *Reynaud et al.* [1995]) and the average seasonal transports [*Lazier and Wright*, 1993; *Han and Tang*, 1999], which suggest a downstream decrease.

[69] There is also some flow over the shelf in the inshore branch of the Labrador Current, inadequately sampled in this data set but known to feed a transport through Belle-Isle Strait north of Newfoundland and along the east coast of Newfoundland. Some of this flow joins the slope branch of the Labrador Current near 49°N [see also *Colbourne et al.*, 1997]. There are also portions of trajectories offshore of the Labrador Current corresponding to a poleward displacement opposite to the Labrador Current (this is vaguely reminiscent of the counterflow observed by float at 700 m by *Lavender et al.* [2000]). The quasi-Eulerian Labrador Current bears much in common with the circulation resulting from the diagnostic analysis of hydrography by *Reynaud et al.* [1995].

[70] The sampling in the Labrador Current is better near 49°N and farther south, which is the region where the USCG International Ice Patrol has been releasing drifters for over 15 years. Just upstream of Flemish Pass, the surface Labrador Current is maximum between the 200 and 2000 m isobaths, whereas in the Flemish Pass at 47°N the flow is mostly between the 200 m to its west side and the maximum depth of the pass (near 1100 m) [see also *Petrie and Buckley*, 1996]. It seems that the flow over deeper isobaths feeds the branch north of the Flemish Cap, with maximum velocities for depths 1000–3000 m (Figure 15b). Some of the trajectories in this flow turn anticylonically around the Flemish Cap before rejoining the Subarctic Front to the east of the Flemish Cap, while some reach it more directly north of the Flemish Cap. Other trajectories separate from that branch

near 47°W and penetrate in the Flemish Pass to continue along the Grand Banks farther south, where the maximum current is over depths 1000–2000 m. Some trajectories continue southward to the vicinity of the tail of the bank near 43°N. A few drifters (most of them drogued at 50 m) originating in the Labrador Current travel around the tail of the Grand Bank and then move to the west-northwest along the continental slope, in three instances to 55°W. These drifters later return eastward and join the NAC system.

5. Conclusions

[71] The velocity and displacement data from the drifters drogued at 15 m provide a unique coverage of a large part of the North Atlantic with a resolution not matched by other means. This produces a fairly detailed mapping of the quasi-Eulerian fields of current and eddy kinetic energy. It illustrates the presence of numerous recirculations, interaction with topography, and quasi-stationary current meanders. Very often the data are sufficient at a resolution on the order of 50 km, sometimes even better where currents are strongly constrained by topography, such as for the currents along the rim of the subpolar gyre. Despite the large number of drifters that were deployed, there are still some areas of relative low data coverage: for instance, in the tropical Atlantic or south of the Gulf Stream. There were also relatively few drifters entering the Gulf Stream from south of Cape Hatteras, which resulted in a bias of the circulation in the Gulf Stream region.

[72] This view of the circulation is derived from drifters with a very inhomogeneous deployment strategy. Such a set may lead to a biased average circulation because drifters tend to congregate in convergent areas and avoid divergent areas. A comparison between quasi-Eulerian and Eulerian estimates of the circulation in a very high resolution model simulation has already been presented by *Garrafo et al.* [2000]. With all the model caveats in their ability to represent ocean physics such comparisons suggest that the quasi-Eulerian fields from the SVP buoy drifts provide a reasonable estimate of the average circulation in the 1990s. We have tried to alleviate the irregular data density by also using data from undrogued drifters, as well as from other sources of drifters of different designs. This required applying corrections on the drifts based on NCEP winds with random errors on resulting velocities of up to 5 cm s^{-1}. These complementary data are slightly more noisy and add to the background EKE, but as they almost double the size of the data set, their net effect is one of reducing the uncertainties on the mean currents and EKE. We have also tested the effect of strongly reducing the weight of drifters deployed in particularly well sampled areas and have found noticeable changes in the current fields, but not to the point of strongly changing the interpretation of the data. These velocities at 15 m are usually fairly indicative of the subsurface currents, as the Ekman velocity at this level is usually only a small fraction of the major currents [*Ralph and Niiler*, 1999].

[73] The trajectories of the drogued drifters bring new information on the near-surface exchanges between the different current systems, in particular, the Gulf Stream and NAC. Although these data are by no means sufficient by themselves, we obtain a picture on how the GS feeds the NAC, how the NAC branches to the interior and to the subpolar gyre, and how the different current systems of the subpolar gyre are connected. However, because of the distribution of the deployments, it remains relatively unclear to what extent the GS feeds into the AC.

[74] The next challenge would be to use these data and complimentary information to investigate seasonal to interannual variability of the circulation. This will require a very different analysis of the data than that presented here because the time distribution of the data in individual regions may not resolve this variability correctly. The period investigated witnessed the transition of ocean forcing from conditions corresponding to a high NAO index before mid-1995 to a very low one for the next year, followed by a nearly-medium NAO index until 1998. NAO variability is known to influence strongly the atmospheric climate in this area, with a clear signature in sea surface temperature and sea level variability. Recently, altimetric sea level data have been used to illustrate changes in the circulation associated with NAO, for instance, in the NAC [*Reverdin et al.*, 1999; *Ducet et al.*, 2000], in the Labrador Current [*Han and Tang*, 1999], in the Norwegian Current [*Mork and Blindheim*, 2000], or in the position of the GS [*Joyce et al.*, 2000; *Frankignoul et al.*, 2001]. For this last instance, there are indications that the GS west of 55°W was on average farther north by close to 100 km between 1990 and early 1996 with respect to the 1960s and has then shifted back to south. Hydrographic data have also suggested large changes in the circulation [*Greatbatch et al.*, 1991; *Curry and McCartney*, 2001], although the conclusions from these investigations as well as from model simulations [*Häkkinen*, 1999; *Eden and Willebrand*, 2001; *Esselborn and Eden*, 2001] need to be confirmed by direct estimates of the surface circulation. The drifter data can complement information from the altimetric sea level data, and the merging of the different data sets to provide precise maps of the absolute currents in the upper ocean should be an important next step for understanding the role of the North Atlantic Ocean in climate change.

Appendix A: Error Estimates

[75] Error estimates are provided on the basis of Lagrangian timescales chosen in the range indicated by *McClean et al.* [2002]. For simplicity we retain 4 days in the zonal direction and 3 days in the meridional direction, although the distribution is fairly variable and anticorrelates somewhat with the distribution of EKE. We also assume that different drifters provide independent estimates of the field. On the basis of these assumptions we estimate the rms random errors on the mean velocity field (Figure A1a). We estimate an "array" bias related to the gradient in the data density bias and the diffusivities [see *Poulain*, 2001] (Figure A1b). (We illustrate those errors for the GS area of Figure 7a). The two error estimates are certainly overestimated near the GS, where the Lagrangian timescales are smaller according to *McClean et al.* [2002] The random errors are large in the poorly sampled areas south of the GS core and south of 40°N between 55° and 60°W and east of 50°W, as is expected on the basis of the data density map (Figure 1a) and the EKE distribution map (Figure 2). They are smaller than the average currents elsewhere. The array bias is very large near the GS, where it would suggest that we overestimate the cross-current component with this quasi-Euler-

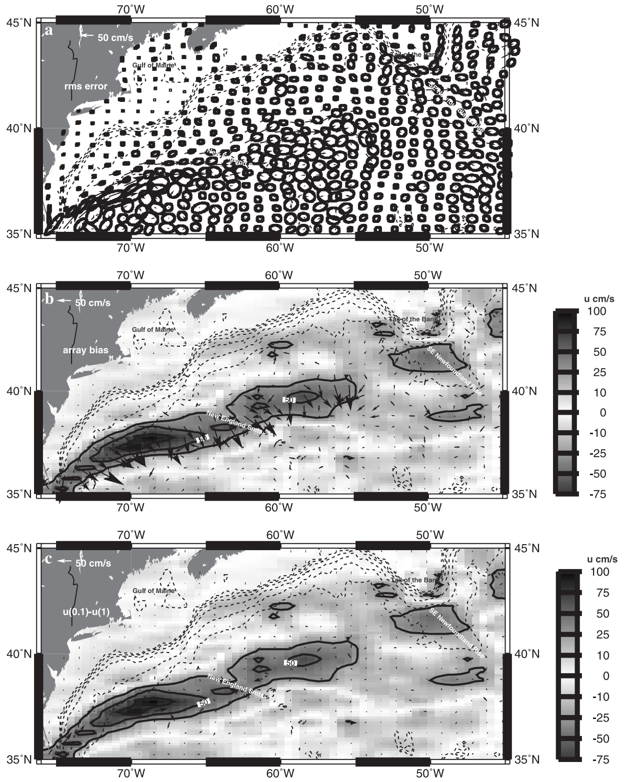

Figure A1. Error estimates: (a) random error ellipses on the average current in the GS area, (b) estimate of array bias, and (c) difference between velocity with weight diminished by 10 for drifters deployed north of the GS and the standard estimate where all drifters have same weight. The contours 25 and 50 cm/s of the zonal current are indicated on Figures A1b and A1c.

ian approach. They are much less than the average currents elsewhere, except maybe for a tendency to have too much divergence of the GS east of 55°W and could contribute to the spread in two branches of the current that we observe.

[76] The magnitude of the estimated array bias is, however, certainly much too large in the GS. We show that by examining the average current of the field where drifters deployed north of the GS are given a lesser weight by a factor 10 compared to the other drifters, which strongly reduces the data density gradient across the GS. The differences between this field and the original field is presented on Figure A1c. The differences are much smaller than the array bias and do not point usually across the GS. This indicates more a change in the average position with a more northerly position of the GS close to Cape Hatteras and a more southerly position near 65°W than what is in the original field. This difference from Figure A1b illustrates that EKE in the GS does not just act to stir the water masses as a purely turbulent flow would, as is assumed in estimating an array bias. A large part of it is in meanders, which still transport the particles in the average current direction (see, e.g., Figure 7c) (at least west of 55°W).

[77] Finally, we will comment the effect of resolution on the estimated EKE. Tests were made lowering the resolution of the grid (1° × 1° or 2° × 1° in latitude × longitude compared to the standart 0.5° × 1° grid). The differences are somewhat noisy but show some systematic differences. In areas of large currents, estimated EKE increases when lowering the resolution: for example, in the GS (37°–38°N, 71°–73°W) it increases from1462 to 1600 cm^{-2} s^{-2} when the resolution goes from 0.5° × 1° to 1° × 2°. This results from including part of the shear in the estimated EKE for the coarser-resolution grid. In areas of weak currents the differences are much more random. Altogether, we do not seem to have underestimated EKE when using the fine resolution despite the often insufficient data coverage. For example, in the eastern Atlantic, 44°–45°N, 15°–19°W, where the data coverage is rather low, EKE is between 76 and 77 cm^{-2} s^{-2} for the three grids. In an area with high data density close to Iceland (61°–62°N, 19°–23°W), EKE is also between 140 and 142 cm^{-2} s^{-2} for the three grids.

[78] **Acknowledgments.** The SVP data originate from a variety of sources, and this common effort to produce such a large data set of Atlantic drifter data is remarkable. Additional complementary data were contributed by D. Murphy at the International Ice Patrol, D. Meldrum at Dunstable Lab. (Scotland), and A. Fiuza at the University of Lisbon (Portugal). One of the authors, Gilles Reverdin, was supported by PNEDC in France. Peter Niiler was supported by Office of Global Programs of NOAA. Sharon Lucas carried the correction of the drifter data for winds at SIO, and Mayra Pazos at AOML/NOAA processed much of the raw ARGOS files into usable numbers. Cedric Lê in 1998 and Virginie Ducros and Jérome Llido in 1999 contributed to the analysis of the data at LEGOS. Discussions with colleagues at CLS, Pierre-Yves Le Traon, Fabrice Hernandez, and Nicolas Ducet were instrumental in pointing out differences between statistics from altimetric and drifter data. Comments by Tom Rossby and one anonymous reviewer were appreciated.

References

Bacon, S., G. Reverdin, I. G. Rigor, and H. M. Snaith, A freshwater jet on the East Greenland shelf, *J. Geophys. Res.*, *107*(C7), 3068, 10.1029/2001JC000935, 2002.

Belkin, I. M., and S. Levitus, Temporal variability of the Subarctic Front near the Charlie-Gibbs Fracture Zone, *J. Geophys. Res.*, *101*, 28,317–28,324, 1996.

Bersch, M., J. Meincke, and A. Sy, Interannual thermohaline changes in the northern North Atlantic 1991–1996, *Deep Sea Res., Part II*, *46*, 55–75, 1999.

Bower, A. S., P. L. Richardson, H. D. Hunt, T. Rossby, M. D. Prater, H.-M. Zhang, S. Anderson-Fontana, P. Perez-Brunius, and P. Lazarevich, Warm-water pathways in the subpolar North Atlantic: An overview of the ACCE RAFOS float programme, *Int. WOCE Newsl.*, *38*, 14–16, 2000.

Brügge, B., Near-surface mean circulation and kinetic energy in the central North Atlantic from drifter data, *J. Geophys. Res.*, *100*, 20,543–20,554, 1995.

Buch, E., Variations in temperature and salinity of west Greenland waters, 1970–1982, *Northwest Atl. Fish. Organ. Sci. Counc. Stud.*, *7*, 39–45, 1984.

Caniaux, G., L. Prieur, H. Giordani, F. Hernandez, and L. Eymard, Observation of the circulation in the Newfoundland Basin in winter 1997, *J. Phys. Oceanogr.*, *31*, 689–710, 2001.

Carr, M.-E., and H. T. Rossby, Pathways of the North Atlantic current from surface drifters and subsurface floats, *J. Geophys. Res.*, *106*, 4405–4419, 2001.

Clarke, R. A., H. W. Hill, R. F. Reiniger, and B. A. Warren, Current system south and east of the Grand Banks of Newfoundland, *J. Phys. Oceanogr.*, *10*, 25–65, 1980.

Colbourne, E., B. deYoung, S. Narayanan, and J. Helbig, Comparison of hydrography and circulation on the Newfoundland shelf during 1990–1993 with the long-term mean, *Can. J. Fish. Aquat. Sci.*, *54*, suppl. 1, 68–80, 1997.

Cuny, J., P. B. Rhines, P. P. Niiler, and S. Bacon, Labrador Sea boundary currents and the fate of Irminger Sea Water, *J. Phys. Oceanogr.*, *32*, 627–647, 2002.

Curry, R., and M. McCartney, Ocean gyre circulation changes associated with the North Atlantic Oscillation, *J. Phys. Oceanogr.*, *31*, 3374–3400, 2001.

Davis, R., Modeling eddy transport of passive tracers, *J. Mar. Res.*, *45*, 635–666, 1987.

Davis, R., Observing the general circulation with floats, *Deep Sea Res., Part A*, *38*, 531–571, 1991.

Davis, R., Preliminary results from directly measuring mid-depth circulation in the tropical and South Pacific, *J. Geophys. Res.*, *103*, 24,619–24,639, 1998.

Ducet, N., and P. Y. Le Traon, A comparison of surface eddy kinetic energy and Reynolds stresses in the Gulf Stream and the Kuroshio Current systems from merged TOPEX/Poseidon and ERS-1/2 altimetric data, *J. Geophys. Res.*, *106*, 16,603–16,622, 2001.

Ducet, N., P. Y. Le Traon, and G. Reverdin, Global high-resolution mapping of ocean circulation from TOPEX/Poseidon and ERS-1/2, *J. Geophys. Res.*, *105*, 19,477–19,498, 2000.

Eden, C., and J. Willebrand, Mechanism of inter-annual to decadal variability of the North Atlantic Oscillation, *J. Clim.*, *14*, 2266–2280, 2001.

Esselborn, S., and C. Eden, Sea surface height changes in the North Atlantic Ocean related to the North Atlantic Oscillation, *Geophys. Res. Lett.*, *28*, 3473–3476, 2001.

Frankignoul, C., G. de Coëtlogon, and T. M. Joyce, Gulf Stream variability and ocean-atmosphere interactions, *J. Phys. Oceanogr.*, *31*, 3516–3529, 2001.

Fratantoni, D. M., North Atlantic surface circulation during the 1990’s observed with satellite-tracked drifters, *J. Geophys. Res.*, *106*, 22,067–22,094, 2001.

Freeland, H. J., P. Rhines, and H. T. Rossby, Statistical observations of trajectories of neutrally buoyant floats in the North Atlantic, *J. Mar. Res.*, *33*, 383–404, 1975.

Garrett, J. F., Availability of the FGGE drifter buoy system data set, *Deep Sea Res., Part A*, *27*, 1083–1086, 1980.

Garraffo, Z. D., A. Griffa, A. J. Mariano, and E. P. Chassignet, Lagrangian data in a high resolution model of the North Atlantic, I, Comparison with in situ drifter data, *J. Mar. Syst.*, *29*, 155–176, 2001a.

Garraffo, Z. D., A. Griffa, A. J. Mariano, and E. P. Chassignet, Lagrangian data in a high resolution model of the North Atlantic, II, On the pseudo-Eulerian averaging of Lagrangian data, *J. Mar. Sys.*, *29*, 177–200, 2001b.

Greatbatch, R. J., A. F. Fanning, A. D. Goulding, and S. Levitus, A diagnosis of interpentadal circulation changes in the North Atlantic, *J. Geophys. Res.*, *96*, 22,009–22,023, 1991.

Häkkinen, S., Variability of the simulated meridional heat transport in the North Atlantic for the period 1951–1993, *J. Geophys. Res.*, *104*, 10,991–11,007, 1999.

Han, G., and C. L. Tang, Velocity and transport of the Labrador Current determined from altimetric, hydrographic, and wind data, *J. Geophys. Res.*, *104*, 18,047–18,057, 1999.

Hansen, D. V., and P.-M. Poulain, Quality control and interpolation of WOCE/TOGA drifter data, *J. Atmos. Oceanogr. Technol.*, *13*, 900–909, 1996.

Helland-Hansen, B., and F. Nansen, The Norwegian Sa: Its physical oceanography based upon the Norwegian researches, 1900–1904, *Rep. 2, Part i (2)*, 390 pp., Norv. Fish. Mar. Invest., Christiana, 1909.

Joyce, T., C. Deser, and M. Spall, Decadal variability of Subtropical Mode Water in the North Atlantic and large-scale patterns of air-sea forcing, *J. Clim.*, *13*, 2550–2569, 2000.

Käse, R. H., and W. Krauss, The Gulf Stream, the North Atlantic Current, and the origin of the Azores Current, in *The Warmwatersphere of the North Atlantic Ocean*, pp. 91–337, Gebrüder Bornträger, Stuttgart, Germany, 1996.

Kearns, E. J., A description of the North Atlantic Current system from historical hydrography, Ph.D. diss., Univ. of R. I., Kingston, 1996.

Kearns, E. J., and H. T. Rossby, Historical position of the North Atlantic Current, *J. Geophys. Res.*, *103*, 15,509–15,524, 1998.

Kelly, K. A., The meandering Gulf Stream as seen by the Geosat altimeter: Surface transport, position, and velocity variance from 73°W to 46°W, *J. Geophys. Res.*, *96*, 16,721–16,738, 1991.

Krauss, W., Currents and mixing in the Irminger Sea and in the Iceland Basin, *J. Geophys. Res.*, *100*, 10,851–10,871, 1995.

Krauss, W., and R. H. Käse, Mean circulation and eddy kinetic energy in the eastern North Atlantic, *J. Geophys. Res.*, *89*, 3407–3415, 1984.

Krauss, W., R. H. Käse, and H. H. Inrichsen, The branching of the Gulf Stream southeast of the Grand Banks, *J. Geophys. Res.*, *95*, 13,089–13,103, 1990.

Lamb, P. J., On the mixed-layer climatology of the north and tropical Atlantic, *Tellus, Ser. A*, *36*, 292–305, 1984.

Lavender, K., R. E. Davis, and W. B. Owens, Mid-depth recirculation observed in the interior Labrador and Irmineger Seas by direct velocity measurements, *Nature*, *407*, 66–69, 2000.

Lazier, J. R. N., Observations in the northwest corner of the North Atlantic Current, *J. Phys. Oceanogr.*, *24*, 1449–1463, 1994.

Lazier, J. R. N., and D. G. Wright, Annual velocity variations in the Labrador Current, *J. Phys. Oceanogr.*, *24*, 1449–1463, 1993.

Lee, T., and P. Cornillon, Temporal variation of meandering intensity and domain-wide lateral oscillations of the Gulf Stream, *J. Geophys. Res.*, *100*, 13,603–13,613, 1995.

Leetmaa, A., P. Niiler, and H. Stommel, Does the Sverdrup relation account for the mid-Atlantic circulation?, *J. Mar. Res.*, *35*, 1–10, 1977.

Lozier, S. M., and G. Gawarkiewicz, Cross-frontal exchange in the Middle Atlantic Bight as evidenced by surface drifters, *J. Phys. Oceanogr.*, *31*, 2498–2510, 2001.

Malmberg, S. A., and H. Valdimarsson, Satellite tracked drifters and “Great Salinity Anomalies” in the subpolar gyre and the Norwegian Sea, *Int. WOCE Newsl.*, *37*, 31–33, 1999.

Mann, C. R., The termination of the Gulf Stream and the beginning of the North Atlantic Current, *Deep Sea Res.*, *14*, 337–359, 1967.

McClean, J. L., P.-M. Poulain, J. W. Peltong, and M. E. Maltrud, Eulerian and Lagrangian statistics from surface drifters and two POP models in the North Atlantic, *J. Phys. Oceanogr.*, in press, 2002.

Mork, K. A., and J. Blindheim, Variations in the Atlantic inflow to the Nordic Seas, 1955–1996, *Deep Sea Res., Part I*, *47*, 1035–1057, 2000.

Niiler, P. P., and J. Paduan, Wind-driven motions in the northeast Pacific as measured by Lagrangian drifters, *J. Phys. Oceanogr.*, *25*, 2819–2830, 1995.

Niiler, P. P., R. E. Davis, and H. J. White, Water-following characteristics of a mixed layer drifter, *Deep Sea Res., Part A*, *31*, 1867–1881, 1987.

Niiler, P. P., A. S. Sybrandy, K. Bi, P. M. Poulain, and D. Bitterman, Measurements of the water-following capability of holey-sock and TRISTAR drifters, *Deep Sea Res., Part I*, *42*, 1951–1964, 1995.

Orvik, K. A., O. Skagseth, and M. Mork, Atlantic inflow to the Nordic Seas: Current structure and volume fluxes from moored current meters, VM-ADCP and SeaSoar-CTD observations, 1995–1999, *Deep Sea Res., Part I*, *48*, 937–957, 2001.

Olson, D., The physical oceanography of two rings observed by the Cyclonic Ring Experiment, part II, Dynamics, *J. Phys. Oceanogr.*, *10*, 514–528, 1980.

Otto, L., and H. M. van Aken, Surface circulation in the northeast Atlantic as observed with drifters, *Deep Sea Res., Part I*, *96*, 467–499, 1996.

Pazan, S. E., and P. P. Niiler, Recovery of near surface velocity from undrogued drifters, *J. Atmos. Technol.*, *18*, 476–489, 2001.

Petrie, B., and J. Buckley, Volume and freshwater transport of the Labrador Current in Flemish Pass, *J. Geophys. Res.*, *101*, 28,335–28,342, 1996.

Pickart, R. S., T. K. McKee, D. J. Torres, and S. A. Harrington, Mean structure and interannual variability of the slopewater system south of Newfoundland, *J. Phys. Oceanogr.*, *29*, 2541–2558, 1999.

Pollard, D. L., and R. T. Regier, Vorticity and vertical circulation at an ocean front, *J. Phys. Oceanogr.*, *22*, 609–625, 1992.

Poulain, P.-M., Adriatic sea surface circulation as derived from drifter data between 1990 and 1999, *J. Mar. Syst.*, *29*, 3–32, 2001.

Poulain, P.-M., and P. P. Niiler, The response of drifting buoys to currents and wind: Comment, *J. Geophys. Res.*, *95*, 797–799, 1990.

Poulain, P. M., A. Warn-Varnas, and P. P. Niiler, Near-surface circulation of the Nordic Seas as measured by Lagrangian drifters, *J. Geophys. Res.*, *101*, 18,237–18,258, 1996.

Ralph, E. A., and P. P. Niiler, Wind-driven currents in the tropical Pacific, *J. Phys. Oceanogr.*, *29*, 2121–2129, 1999.

Reverdin, G., and F. Hernandez, Variability of the Azores Current during October–December 1993, *J. Mar. Syst.*, *29*, 101–123, 2001.

Reverdin, G., N. Verbrugge, and H. Valdimasson, Upper ocean variability between Iceland and Newfoundland 1993–1997, *J. Geophys. Res.*, *104*, 29,599–29,661, 1999.

Reynaud, T. H., A. J. Weaver, and R. J. Greatbatch, Summer mean circulation of the northwestern Atlantic Ocean, *J. Geophys. Res.*, *100*, 779–816, 1995.

Richardson, P. L., Eddy kinetic energy in the North Atlantic from surface drifters, *J. Geophys. Res.*, *88*, 4355–4367, 1983.

Rossby, T., The North Atlantic Current and surrounding waters: At the crossroads, *Rev. Geophys.*, *34*, 463–481, 1996.

Rossby, T., On gyre interactions, *Deep Sea Res., Part II*, *46*, 139–164, 1999.

Rossby, T., and E. Gottlieb, The Oleander project: Monitoring the variability of the Gulf Stream and adjacent waters between New Jersey and Bermuda, *Bull. Am. Meteorol. Soc.*, *79*, 5–18, 1998.

Schmitz, W. J., and M. S. McCartney, On the North Atlantic circulation, *Rev. Geophys.*, *31*, 29–49, 1993.

Stammer, D., Steric and wind-induced changes in TOPEX/Poseidon large-scale sea surface topography variations, *J. Geophys. Res.*, *102*, 20,987–21,009, 1997.

Stommel, H., P. Niiler, and D. Anati, Dynamic topography and recirculation of the Gulf Stream, *J. Mar. Res.*, *36*, 449–468, 1978.

Sy, A., U. Shcauer, and J. Meincke, The North Atlantic Current and the associated hydrographic structure above and eastward of the Mid-Atlantic Ridge, *Deep Sea Res., Par A*, *39*, 825–853, 1992.

Sybrandy, A. L., and P. P. Niiler, WOCE/TOGA Lagrangian drifter construction manual, *SIO Ref. 91/6*, *WOCE Rep. 63*, 58 pp., Scripps Inst. of Oceanogr., La Jolla, Calif., 1991.

Valdimarsson, H., and S. A. Malmberg, Near-surface circulation in Icelandic waters derived from satellite-tracked drifters, *Rit Fiskideildar*, *16*, 23–29, 1999.

Van Meurs, P., and P. P. Niiler, Temporal variability of the large-scale geostrophic surface variability in the northeast Pacific, *J. Phys. Oceanogr.*, *27*, 2288–2297, 1997.

White, M. A., and K. Heywood, Seasonal and interannual changes in the North Atlantic subpolar gyre from Geosat and TOPEX/Poseidon altimetry, *J. Geophys. Res.*, *100*, 24,931–24,941, 1995.

Wunsch, C., The vertical partition of oceanic horizontal kinetic energy, *J. Phys. Oceanogr.*, *27*, 1770–1794, 1997.

Zhou, M., J. Paduan, and P. P. Niiler, The surface currents in the Canary Basin from drifter observations, *J. Geophys. Res.*, *105*, 21,893–21,910, 2000.

P. P. Niiler, Scripps Institution of Oceanography, University of California, San Diego, 9500 Gilman Drive, Mail Code 0230, La Jolla, CA 92093-0230, USA.

G. Reverdin, LODYC, 4 Pl. Jussieu, 75005 Paris, France. (gilles.reverdin@lodyc.jussieu.fr)

H. Valdimarsson, Marine Research Institute, P. O. Box 1390, Skulagata 4, 121 Reykjavik, Iceland.

Figure 2. (opposite) Map of EKE with average current and bathymetry (contours 200, 1000, 2000, 3000, and 4000 isobaths): (a) the northern and (b) the southern portions of the North Atlantic. The color scale is on the right.

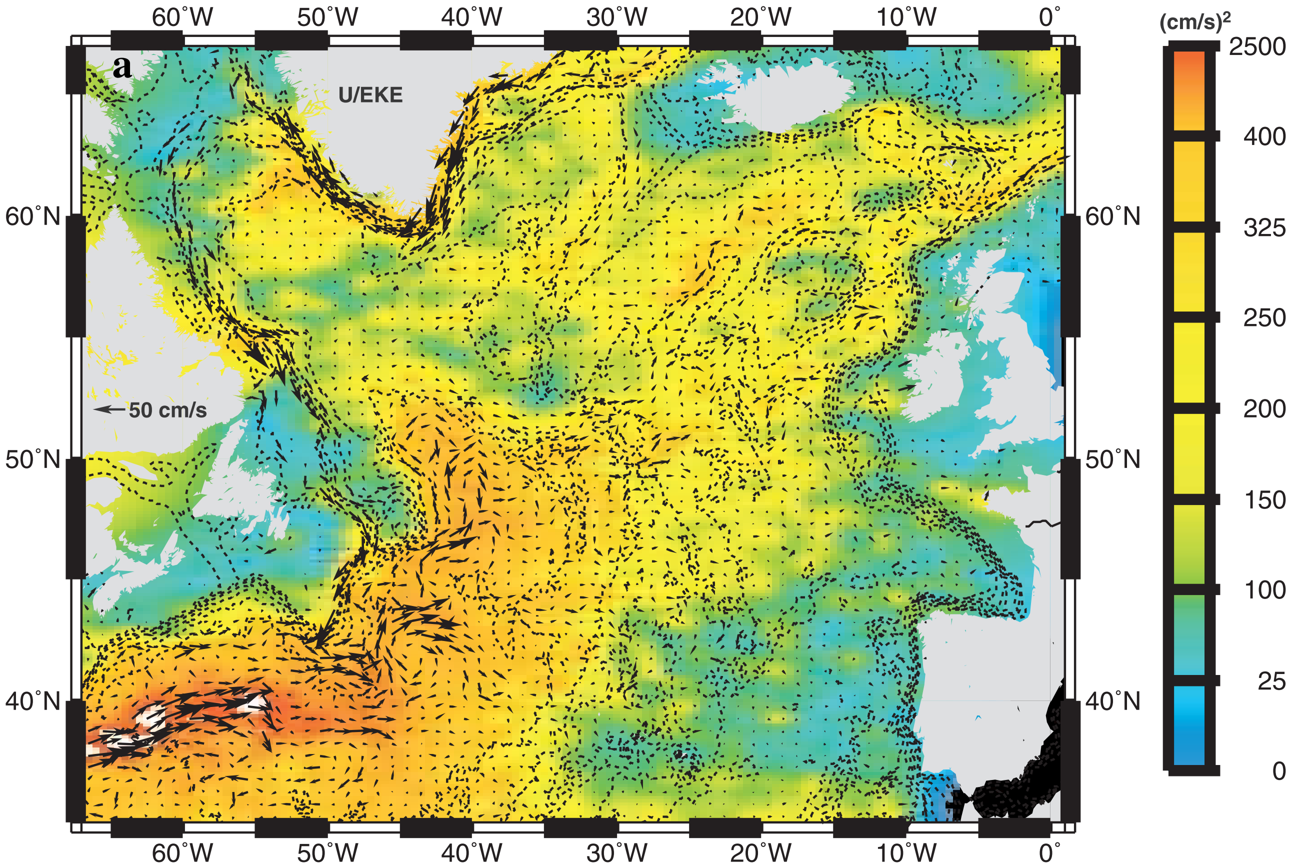
a
U/EKE
50 cm/s
60˚W
50˚W
40˚W
30˚W
20˚W
10˚W
0˚
60˚N
50˚N
40˚N
(cm/s)^2
2500
400
325
250
200
150
100
25
0

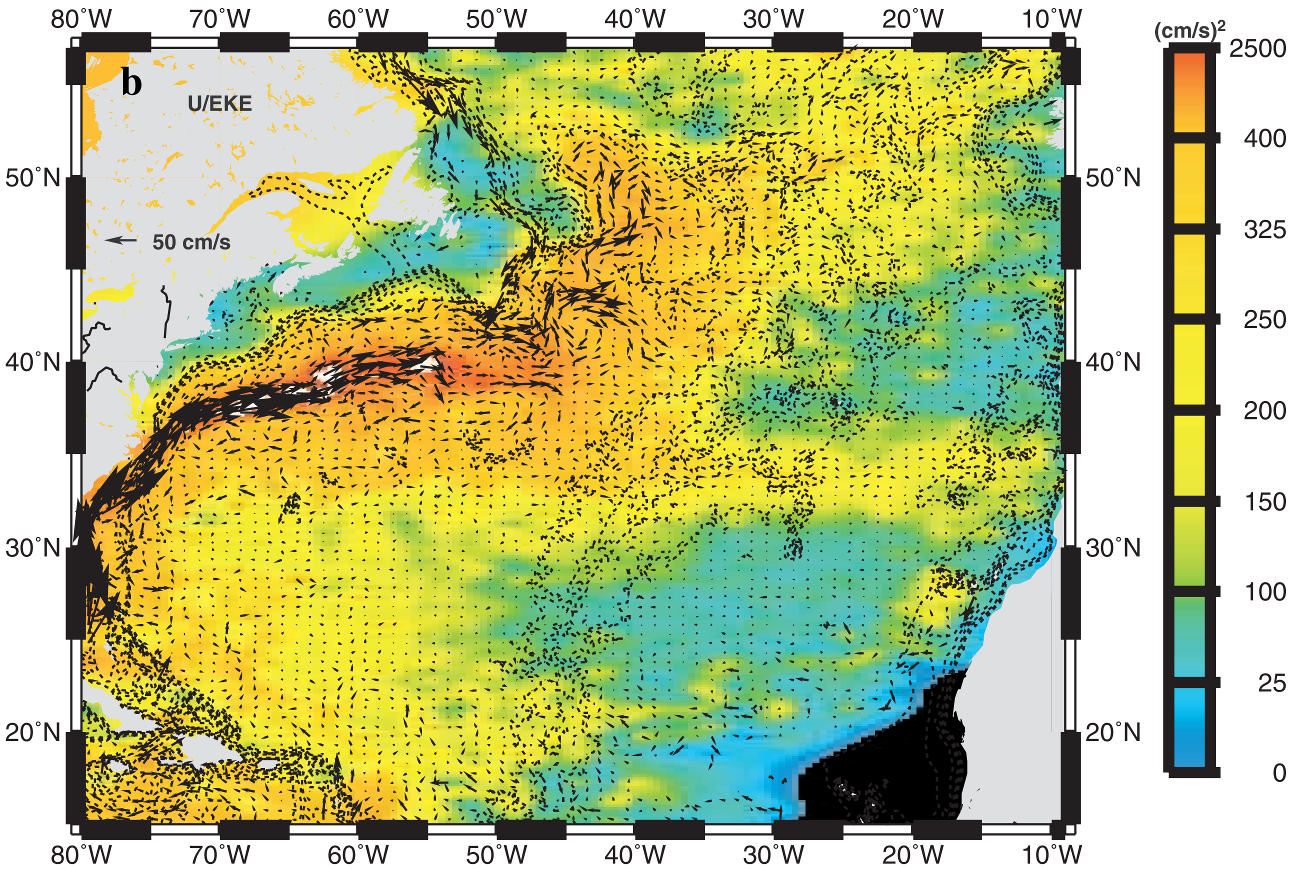
b
U/EKE
50 cm/s
80˚W
70˚W
60˚W
50˚W
40˚W
30˚W
20˚W
10˚W
50˚N
40˚N
30˚N
20˚N
(cm/s)^2
2500
400
325
250
200
150
100
25
0